caption

VECTOR-BORNE PATHOGEN AND HOST EVOLUTION IN A STRUCTURED IMMUNO-EPIDEMIOLOGICAL SYSTEM

HAYRIYE GULBUDAK*, VINCENT L. CANNATARO, NECIBE TUNCER, AND MAIA MARTCHEVA

Abstract. Vector-borne disease transmission is a common dissemination mode used by many pathogens to spread in a host population. Similar to directly transmitted diseases, the within-host interaction of a vector-borne pathogen and a host's immune system influences the pathogen's transmission potential between hosts via vectors. Yet there is much less theoretical studies on virulence-transmission tradeoffs and evolution in vector-borne pathogen-host systems. Here we consider an immuno-epidemiological model that links the within-host dynamics to between-host circulation of a vector-borne disease. On the immunological scale, the model mimics antibody-pathogen dynamics for arbovirus diseases, such as Rift Valley Fever and West Nile Virus. The within-host dynamics govern transmission and host mortality and recovery in an age-since-infection structured host-vector-borne pathogen epidemic model. By considering multiple pathogen strains and multiple competing host populations differing in their within-host replication rate and immune response parameters, respectively, we derive evolutionary optimization principles for both pathogen and host. Invasion analysis shows that the $\mathcal{R}_0$ maximization principle holds for the vector-borne pathogen. For the host, we prove that evolution favors minimizing case fatality ratio (CFR), which is consistent with a very recent work by Martcheva et al. [14]. These results are utilized to compute host and pathogen evolutionary trajectories, and to determine how model parameters affect evolution outcomes. We find that increasing the vector inoculum size increases the pathogen $\mathcal{R}_0$, but can either increase or decrease the pathogen virulence (the host CFR), suggesting that vector inoculum size can contribute to virulence of vector-borne diseases in distinct ways.

Keywords: immuno-epidemiological modeling, Rift Valley Fever, West Nile Virus, vector-borne pathogen, differential equations, reproduction number, vector incoulum size, age-since-infection, within-host dynamics, coevolutionary attractor, tradeoffs.

AMS Subject Classification: 92D30, 92D40

1. Introduction

Parasites and hosts exert *selective pressure* on each other, leading to reciprocal adaptation. This phenomenon is a driving force in important topics such as how to control epizootics in nature, the source of new strains, and the mechanisms behind evolving host resistance and parasite virulence. Many medically relevant diseases are caused by coevolving parasites, making understanding the evolution and coevolution of host and parasites in general very important [16]. Although there are empirical studies, only a scare amount of them manage to explicitly study the virulence of viruses to test hypotheses on the evolution of pathogen virulence [35, 36]. As a result, many theoretical studies have been motivated by the questions: Why do parasites harm their hosts? What is the

Date: October 30, 2016.

*author for correspondence.

evolutionary trajectory of virus strategy? The tradeoff between virulence and the transmission has been studied extensively by many researchers [21, 13, 57, 58, 60]. Later these studies extended to host evolution since its know that parasites exert selective pressure on their hosts[39].

Early models of host-pathogen evolution, reviewed in [21], were mostly systems of ODEs and studied tradeoffs between transmission and virulence with specifying a priori particular trade-off between epidemiological parameters. Bremermann and Thieme [24] provided rigorous support for the principle of $\mathcal{R}_0$ maximization, i.e. pathogens evolve toward maximizing their reproduction number, by proving competitive exclusion in a general multi-strain SIR model. These and similar results have been utilized by other researchers to explore evolution of virulence [21, 13, 57, 58, 60]. Gilchrist and Sasaki [17] introduced a nested modeling approach which directly displayed the transmission-virulence tradeoff by explicitly linking an epidemiological model for directly transmitted pathogens to a within-host system depicting simple pathogen-immune dynamics. In addition, the within-host model can potentially be parameterized using data collected for individual-level experiments, thereby allowing extrapolation to the between-host level on the basis of empirical data [49]. Moreover, linking within-host and between-host scales offers a natural setting for investigating the evolution of both pathogen and host.

In addition to employing the principle of $\mathcal{R}_0$ maximization for pathogen evolution, Gilchrist and Sasaki [17] used the *lifespan of the host* in the infectious class as a criterion for host evolution, assuming no natural mortality. Pugliese [15] later analytically show that, even in the presence of natural mortality, the host evolves towards maximizing its lifespan in the infectious class. Bowers [41] derived a principle for host evolution states that the host evolves toward minimizing a dimensionless quantity called the basic depression number D_0. In a very recent work, Martcheva et al. [14] show that for the directly transmitted diseases with recovery or chronic infection mode, the host evolves toward minimizing its case fatality ratio (CFR). However, evolution of both host and pathogen has not been investigated in the context of *vector-borne pathogen* transmitted diseases.

Vector-borne disease spread is the most common dissemination mode, causing many diseases and epidemics in the history. A vast majority of vector-borne vertebrate-infecting viruses (arboviruses) are responsible for a number of severe diseases in humans (yellow fever, dengue, various encephalitides, etc.) and livestock (West Nile encephalomyelitis, Rift Valley fever, vesicular stomatitis, etc.). So in general it is important to understand how vector-borne pathogens evolve. In verbal arguments, Ewald [37, 38] suggested that due to the mobility of their intermediate hosts such as mosquitos, flees, etc., vector-borne pathogens might evolve toward higher virulence. Then in a theoretical study, in response to this claim, Day [50] provided an alternative hypothesis, suggesting that the vector-born pathogen virulence evolution may depend on vector inoculum size. Yet, there has not been a sophisticated vector-host model that links within-host and epidemiological dynamics and investigates how vector inoculum size affects the evolution of vector-borne diseases. Here we provide a nested approach to study vector-borne pathogen and host evolution, allowing us to examine virulence evolution in response to vector inoculum size.

The existing theoretical studies in vector-borne diseases only focus on viral evolution and show $\mathcal{R}_0$ maximization under limited assumptions [25, 30]. However none of the

studies have been extended to co-evolution of hosts in response to vector-borne parasite infection. Here in this study, we ask: what are the optimal evolutionary host and virus strategies and how vectors can influence coevolutionary trajectories of host and parasites? In particular, we obtain the evolutionary principle of CFR minimization for hosts by analyzing an infection-age structured vector-borne epidemiological model with multiple competing host populations with distinct immunological traits (analogously we obtain pathogen evolutionary principle; $\mathcal{R}_0$ maximization). Furthermore, with our established fitness optimization principles, we compute evolutionary trajectories of the host immune defense trait and within-host pathogen replication rate. This allows us to detail how relevant within-host parameters, in the paradigm of vector-borne diseases, affect pathogen-host evolution; in particular, we determine the impact of vector inoculum size on evolution of virulence.

The paper is organized as follows: In Section 2, we introduce a structured immunoepidemiological vector-host model, in which the epidemic parameters are governed by the arbovirus within-host pathogen-immune response. In our immunological system, we incorporate the specific antibody dynamics that are most measured in the laboratory and the field and utilize vector-host disease transmission, which pertains particularly well to arbovirus diseases, such as Rift Valley Fever (RVF), Dengue, and West Nile Virus (WNV), mosquito-borne diseases infecting many different mammal species, including livestock and humans [3, 1]. In Section 3, we rigorously derive the host evolution criterium and virus criterium by vector-borne diseases. Through numerical approaches, we investigate the co-evolutionary evolutionarily stable strategies of both host and their viruses, in particular exploring how variable vector inoculum size affects evolution of virulence. In the last section, we discuss our results.

2. Immuno-Epidemiological Modeling In Vector-Host Sytems

2.1. **Immunological scale pathogen-immune Interactions.** Mammals have a humoral immune system which responds to pathogen invasion by creating memory cells and antibodies. These components of the immune system decrease the waiting time of an immune response upon subsequent exposure to additional pathogen. Typically, once immune cells learn the structural make up of an invading pathogen, they can produce antibodies that are specific to the pathogen and bind to the pathogen, signaling for rapid destruction. Initially during a viral infection, there is a rapid production of Immunoglobulin M (IgM) antibodies, followed by a longer lasting production of Immunoglobulin G (IgG) antibodies [33]. These two antibodies are often measured in laboratory settings to determine how a host is fighting an administered pathogen.

Here we develop an immunological model (2.1) describing the interaction between pathogen and IgM, IgG immune response antibodies. $M(\tau)$ and $G(\tau)$ denote the within-host IgM and IgG antibody concentrations at time-since-infection τ , respectively. We assume that the pathogen, $P(\tau)$, replicates with a rate r. IgM and IgG immune response antibodies contribute to the elimination of the pathogen at rates ϵ and δ, respectively. The IgM immune response antibodies proliferate at a rate proportional to the viremia level in the host, represented by the activation rate a, and decays at rate c. The IgM immune response antibodies are mainly responsible for rapid destruction of invading pathogen. B cells switch production of IgM immune response antibodies to production of a longer lasting class, IgG, at rate q. IgG immune response antibodies activate at

a per-capita rate b. The definition of parameters and variables for our immunological model are given in Table 1. This within-host pathogen-immune response dynamics are described by the coupled differential equations:

$$\begin{cases} \dfrac{dP}{d\tau} = (r - \epsilon M(\tau) - \delta G(\tau))P(\tau) \\ \dfrac{dM}{d\tau} = aM(\tau)P(\tau) - (q+c)M(\tau) \\ \dfrac{dG}{d\tau} = qM(\tau) + bG(\tau)P(\tau). \end{cases} \tag{2.1}$$

In the absence of immune response ($M_0 = 0, G_0 = 0$), the pathogen grows exponentially, in which case it is expected that the infected host dies since the parasite damages the host. However, when immune response is active ($M_0 > 0$ or $G_0 > 0$), then the pathogen eventually clears ($\lim_{\tau\to\infty} P(\tau) = 0$), the IgM immune response antibodies decays to zero after viral clearance and subsequently the IgG immune memory antibodies reach a steady-state; i.e. $\lim_{\tau\to\infty} M(\tau) = 0$ and $\lim_{\tau\to\infty} G(\tau) = G^*$, where $G^* > 0$ (See Appendix). The Figure (1) illustrates the within-host pathogen-immune response antibody dynamics.

TABLE 1. Definition of the variables in the within-host modeling framework

Variable/Parameter	Meaning
$P(\tau)$	Pathogen concentration at τ days postinfection
$M(\tau)$	The concentration of IgM immune response antibodies at infection age τ,
$G(\tau)$	The concentration of IgG immune memory antibodies at infection age τ,
r	Parasite growth rate,
ϵ	The efficiency of the IgM immune response at killing the parasite,
δ	The efficiency of the IgG immune response at killing the parasite,
a	The IgM immune response activation rate,
q	The per-capita rate at which the IgM immune response antibody production switches to the IgG immune response antibody production,
b	The IgG activation rate upon coming into contact with the pathogen,
c	IgM immune response antibody decay rate,

2.2. **Epidemiological scale between-host transmission.** In epidemiological setting, we introduce *an age-since infection structured vector-host model,* in which vectors are the only mechanism transmitting the disease to susceptible hosts and the infected host compartment is structured by age-since-infection τ. τ indicates the time passed after

infection. In the host model, $S(t), I(t), R(t)$ denote the total number of susceptible, infected and recovered host population at time t, respectively, and in the vector model, $S_V(t), I_V(t)$ indicate the number of susceptible and infected vectors, respectively. The host population has growth rate $f(N)$, where $f(N)$ is a function of the total population size, $N = S+I+R$. We utilize the logistic growth term $f(N) = \tilde{b}N(1-\frac{N}{K})$, with carrying capacity K and net growth rate $\tilde{b}$ Logistic growth rate in the host population provides a good foundation for host competition, which is used to investigate host evolution in the next section in a multi-host version of the vector-host age-since-infection structured model (see (3.2). In the model, $i(\tau, t)$ represents the density of infected hosts who have infection age τ at time t. A portion of the susceptible hosts move to the infected compartment with a rate $\beta_1 I_V(t)$ through a bite by an infected vector I_V. Infected hosts recover with a rate γ and die due to natural causes with a rate d and due to disease with a rate α (death due to pathogen resource use) and κ (due to immune cell resource use).

$$
\begin{cases}
\dfrac{dS}{dt} &= f(N(t)) - \beta_1 S(t) I_V(t) - dS(t) \\
\dfrac{\partial i}{\partial t} + \dfrac{\partial i}{\partial \tau} &= -(\alpha(\tau) + \kappa(\tau) + \gamma(\tau) + d) i(\tau, t), \\
i(0, t) &= \beta_1 S(t) I_V(t), \\
\dfrac{dR}{dt} &= \displaystyle\int_0^\infty \gamma_i(\tau) i(\tau, t) d\tau - dR(t),
\end{cases} \tag{2.2}
$$

Integrating with respect to τ over the density $i(\tau, t)$ of infected host population with infection age τ at time t, we obtain the total infected host population at time t,

$$I(t) = \int_0^\infty i(\tau, t) d\tau.$$

Moreover, a portion of the susceptible vectors move to the infected vector compartment with a rate $S_V(t) \displaystyle\int_0^\infty \beta_H(\tau) i(\tau, t) d\tau$. The parameter η gives vector birth rate and vectors leave the compartment with a natural death rate μ. The vector model is as follows:

$$
\begin{cases}
\dfrac{dS_V}{dt} = \eta - S_V(t) \displaystyle\int_0^\infty \beta_H(\tau) i(\tau, t) d\tau - \mu S_V(t), \\
\dfrac{dI_V}{dt} = S_V(t) \displaystyle\int_0^\infty \beta_H(\tau) i(\tau, t) d\tau - \mu I_V(t),
\end{cases} \tag{2.3}
$$

The definitions of parameters and variables for the vector-host model are given in Table 2.

To link epidemiological parameters to within-host pathogen-immune dynamics, we assume a simple form of disease induced death rates $\alpha + \kappa$, depending on infection age τ, (similar to [17]) that is,

$$\alpha(\tau) = r\sigma P(\tau) \text{ and } \kappa(\tau) = a\nu M(\tau) P(\tau),$$

where $\alpha(\tau)$ represents host mortality due to the pathogen and $\kappa(\tau)$ gives the additional host mortality due to the immune response and σ, ν are cost coefficients. The transmission rate $\beta(\tau)$ is also dependent on the within-host pathogen load. Here, as

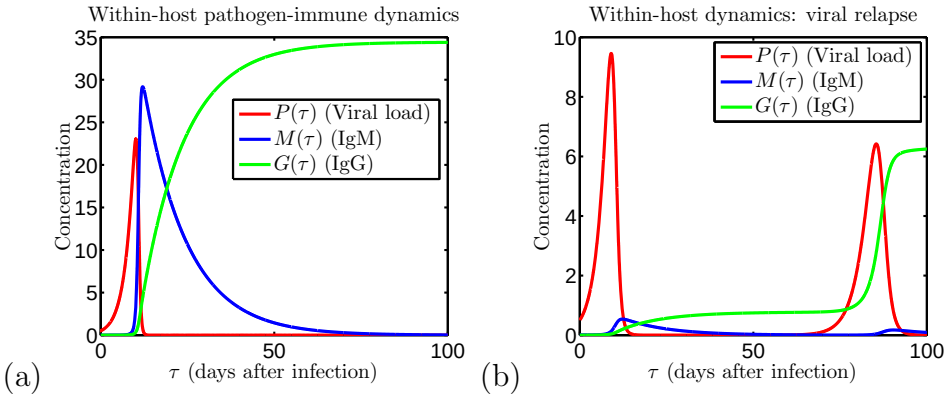

FIGURE 1. *Distinct within-host pathogen-immune response antibody dynamics* (a) An increase in viral load triggers an immune response of IgM which causes the viremia levels to drop, and persistence of long-term immunity by IgG follows after host clears the virus. Immuniological model parameter values for the simulation are: $r = 0.4,\ \epsilon = 0.1,\ \delta = 0.1,\ a = 0.1,\ q = 0.08,\ c = 0.000002$ and $b = 0.04$. Immunological model initial values are $P(0) = 0.5,\ M(0) = 0.01,\ G(0) = 0.001$ (b) In this simulation, an immune response of IgM drops the viremia level. However the immune system does not handle the virus well enough and a rebound in viremia load occurs. In the second phase of the infection which starts after viral rebound, the IgG immune memory response kill the rest of virus population. The immunological parameter values are identical to the parameter values in part (a), except $\epsilon = 3$. We observe that increasing the IgM immune response killing efficacy parameter, ϵ, increases the likelihood of viral relapse.

data suggested [11, 10, 12], we formulate the transmission rate $\beta(\tau)$ as Holling type II function with respect to the pathogen load $P(\tau)$ at a given time-since-infection τ:

$$\beta(\tau) = \phi \frac{P^2(\tau)}{C_0 + P^2(\tau)}, \tag{2.4}$$

where $C_0,\ \phi$ are half saturation and transmission constants, respectively.

Here, we formulate the recovery rate $\gamma(\tau)$ as a function of immune response $G(\tau)$ and inversely related to the viral load:

$$\gamma(\tau) = \psi \frac{G(s)}{G(s) + \epsilon_0} e^{-P(\tau)},$$

where $\epsilon_0 > 0$ is proportionality constant and a small number. In our modeling framework, this notion of recovery translates into low pathogen load with sufficient IgG memory antibodies to prevent subsequent rise in pathogen load. Therefore recovery rate should be a decreasing function of $P(\tau)$ and increasing function of $G(\tau)$. While a simpler form of $\gamma(\tau)$ can be specified with these properties [1], we utilize the above form of $\gamma(\tau)$ in order to reduce sensitivity of the recovery rate to the magnitude of the within-host variables. Here, as $P(\tau)$ decreases to zero and $G(\tau)$ reaches a large enough level,

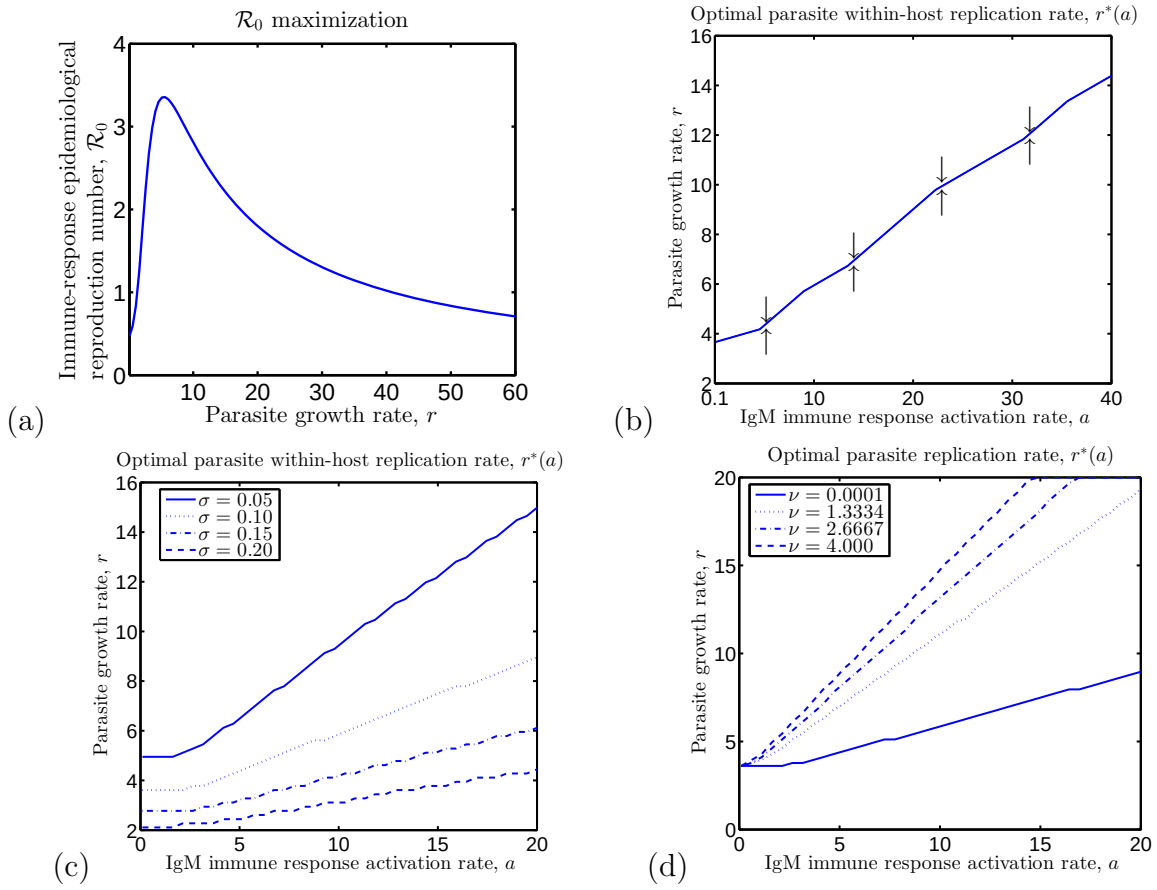

FIGURE 2. *Parasite evolution, with trait r, w.r.t. costly immune response and parasite invasion cost. a) $\mathcal{R}_0$ maximization at an intermediate parasite growth rate r. b) Parasite optimality curve, $r^*(a)$, vs. a. Here the cost coefficients are fixed at $\sigma = 0.1$ and $\nu = 0.0009$. c) Optimal replication rate curve, $r^*(a)$, vs. host immune response rate a, for various values of the parasite damage coefficient σ and the host immune response coefficient ν (d).The epidemiological model parameter values: $\tilde{b} = 1$, $K = 36500$ (in units 10^4 hosts per day), $\mu = 1/10$, $\eta = 0.02$ (in units 10^8 vectors per day), $d = 1/(365 \times 10), \beta_1 = 1$. The linking parameter constants and the values of the remaining linking parameters are $\phi = 0.03$, $C_0 = 100$, $\psi = 2$, $\epsilon_0 = 1$.*

the recovery rate increases to a maximum rate ψ. The term

$$1 - e^{-\int_0^\tau \gamma(s)ds},$$

gives the probability of being recovered at infection age τ assuming that individuals can only leave the infected compartment through recovery. Definitions of the parameters linking within-host and between host model are given in Table 3.

The *immune-response dependent epidemiological reproduction number* is given by:

TABLE 2. Definition of the variables in the between-host modeling framework

Variable/Parameter	Meaning
$S_V(t)$	The number of susceptible vectors at time t,
$I_V(t)$	The number of infected vectors at time t,
$S(t)$	The number of susceptible individuals at time t,
$i(\tau, t)$	The density of the infected individuals with infection age τ at time t,
$R(t)$	The number of recovered individuals at time t,
$f(N)$	Host recruitment rate as a function of total host population N
η	Susceptible vector recruitment rate
β_1	Infected vector transmission rate
$\beta(\tau)$	Infected individual transmission rate at τ days postinfection
$\alpha(\tau)$	Additional host mortality rate due to parasite resource use at τ days postinfection
$\kappa(\tau)$	Additional host mortality rate due to immune response resource use at τ days postinfection
$\gamma(\tau)$	Per capita host recovery rate τ days postinfection
d	Host natural death rate
μ	Vector natural death rate

TABLE 3. Definition of the parameters in linking within-host & between-host modeling frameworks

Variable/Parameter	Meaning
σ	the parasite cost coefficient,
ϕ	the transmission efficiency of the parasitic infection,
ν	the immune response cost coefficient,
C_0	half-saturation constant in transmission rate,
ψ	saturation constant in recovery rate,
ϵ_0	half-saturation constant in recovery rate,

$$\mathcal{R}_0 = \frac{\beta_1 S^0}{\mu} \cdot \int_0^\infty S_V^0 \beta_j(\tau) e^{-\int_0^\tau (\alpha(s)+\kappa(s)+\gamma(s)+d)ds} d\tau,$$

where $S^0 = K(1 - \frac{d}{\tilde{b}})$. The constant $\frac{\beta_1 S^0}{\mu}$ in $\mathcal{R}_0$ represents the average number of secondary infected hosts produced by one infected vector during its infectious time

period among the whole susceptible host population. The term $S_V^0\beta_j(\tau)$ in $\mathcal{R}_0$ gives the number of secondary infected vectors produced by one infectious host at infection age τ among the whole susceptible vector population. The integral

$$\int_0^\infty S_V^0\beta(\tau)e^{-\int_0^\tau(\alpha(s)+\kappa(s)+\gamma(s)+d)ds}d\tau$$

accumulates all those quantities for all infection statuses of the host and gives the average number of secondary infected vectors produced by one infected host during its infectious time period when it is introduced into a completely susceptible vector population. The basic reproduction number $\mathcal{R}_0$ keeps track of the number of secondary infectious hosts produced by one infected host during its infectious time period in an entirely susceptible host population. Also the terms $e^{-\int_0^\tau(\alpha(s)+\kappa(s)+\gamma(s))ds}$, $e^{-d\tau}$ give the probability of still being infected at infection age τ and the probability of having survived to infection age τ, respectively.

The reproduction number $\mathcal{R}_0$ represents both a threshold between extinction and persistence, and a measure of fitness, for the pathogen. Here, we summarize the role of $\mathcal{R}_0$ in determining existence and stability of an endemic equilibrium of model (2.2) with constant host growth rate $f(N) = \Lambda$. For the system with a constant host growth rate, the analysis of the population dynamics is summarized as follows: The reproduction number $\mathcal{R}_0$ is strict threshold for disease eradication. Whenever $\mathcal{R}_0 < 1$, the disease free equilibrium is globally asymptotically stable; i.e the disease always eradicate whenever $\mathcal{R}_0$ is below unity. However when $\mathcal{R}_0 > 1$, the endemic equilibrium $\mathcal{E}^* = (S_H^*,\ i_H^*(\tau),\ R_H^*,\ S_V^*,\ I_V^*)$ (when $f(N) = \Lambda$,) where

$$S_H^* = \frac{1}{\beta_1\dfrac{S_V^*}{\mu}\displaystyle\int_0^\infty\beta(\tau)\pi(\tau)d\tau},\ i_H^*(\tau) = i_H^*(0)\pi(\tau),\ R_H^* = \frac{i_H^*(0)}{d}\int_0^\infty\gamma(\tau)\pi(\tau)d\tau,$$

$$S_V^* = \frac{\eta}{i_H^*(0)\displaystyle\int_0^\infty\beta(\tau)\pi(\tau)d\tau+\mu},\ I_V^* = \frac{S_V^*}{\mu}\int_0^\infty\beta(\tau)i_H^*(\tau)d\tau,$$

with

$$\pi(\tau) = e^{-d\tau-\int_0^\tau(\alpha(s)+\kappa(s)+\gamma(s))\,ds},\qquad i_H^*(0) = \frac{\Lambda}{d}\frac{\left(1-\dfrac{1}{\mathcal{R}_0}\right)}{\left(\dfrac{1}{d}+\dfrac{\mu}{\beta_1\eta}\right)},$$

is globally asymptotically stable [45].

Although the vector-host system with constant host growth rate is a simpler model to investigate the evolution of virus, it is not a good choice for studying the host evolution, since the system can not account for host competition. Thus, the logistic growth, $f(N) = \tilde{b}N(1-\dfrac{N}{K})$, will be utilized in our study. A major difficulty arises when analyzing the stability of positive equilibria of the system because of the assumed logistic growth in the

host population. Therefore we introduce the following conditions which ensure stability of the endemic equilibrium.

Define

$$\tilde{T_0} = \tilde{b}(1 - \frac{2N_1^*}{K}),$$
$$\hat{T}(\lambda) = 1 - \tilde{T_0}\int_0^\infty (1 + \frac{\gamma_1(\tau)}{\lambda + d})e^{-\lambda\tau}\pi_1(\tau)d\tau,$$

where $N_1^* = S_H^* + I_{H_1}^* + R_H^*$ and $\hat{T}(\lambda)$ is a complex function.

Suppose that for any λ with $\Re\lambda \geq 0$ we have:

$$\Re\hat{T} \geq 0, \qquad \Im\hat{T} \geq 0, \qquad and \qquad d - \tilde{T_0} > 0. \tag{2.5}$$

The following theorem (proof in Appendix) characterizes existence and stability of an endemic equilibrium for the system (2.2):

Theorem 2.1. *If $\mathcal{R}_0 > 1$, then there exists an endemic equilibrium $\mathcal{E}$. If we assume, furthermore, that condition (2.5) holds, then $\mathcal{E}$ is locally asymptotically stable.*

3. Pathogen and Host Evolution in Nested Vector-Borne Disease Model

3.1. **Pathogen evolution: $\mathcal{R}_0$ maximization.** To study the pathogen evolution in vector-host systems with limited resources, we describe one host-one vector-two strain immuno-epidemiological system:

$$\begin{cases} \dfrac{dS_H}{dt} &= f(N) - S_H(t)\displaystyle\sum_{i=1}^{2}\beta_{v_i}I_{V_i}(t) - dS_H(t) \\ \dfrac{\partial i_{H_i}}{\partial t} + \dfrac{\partial i_{H_i}}{\partial \tau} &= -(\alpha_i(\tau) + \kappa_i(\tau) + \gamma_i(\tau) + d)i_{H_i}(\tau,t), \\ i_{H_i}(0,t) &= \beta_{v_i}S_H(t)I_{V_i}(t), \\ \dfrac{dR_H}{dt} &= \displaystyle\sum_{i=1}^{2}\int_0^\infty \gamma_i(\tau)i_{H_i}(\tau,t)d\tau - dR_H(t), \\ \dfrac{dS_V}{dt} &= \eta - S_V(t)\displaystyle\sum_{i=1}^{2}\int_0^\infty \beta_{h_i}(\tau)i_{H_i}(\tau,t)d\tau - \mu S_V(t), \\ \dfrac{dI_{V_i}}{dt} &= S_V(t)\displaystyle\int_0^\infty \beta_{h_i}(\tau)i_{H_i}(\tau,t)d\tau - \mu I_{V_i}(t), \end{cases} \tag{3.1}$$

where $N = S_H + I_{H_1} + I_{H_2} + R_H$ with $I_{H_i} = \displaystyle\int_0^\infty i_{H_i}(\tau,t)d\tau$.

The existence of single strain type j equilibria is equivalent to existence of the endemic equilibrium $\mathcal{E}$ in the underlying single host model. Indeed, if the reproduction number for strain j is greater than one; i.e. $\mathcal{R}_j > 1$, then the two-strain model (3.2) has a unique single strain type j equilibrium $\mathcal{E}_j$, where $\mathcal{E}_1 = (S_H^*, i_{H_1}^*(\tau), 0, R_H^*, S_V^*, I_{V_1}^*, 0)$ and $\mathcal{E}_2 = (S_H^*, 0, i_{H_2}^*(\tau), R_H^*, S_V^*, 0, I_{V_2}^*)$ (See the proof (6.2) in Appendix).

We investigate pathogen evolution through considering Adaptive Dynamics approach. A rare mutant strain, V_2, can invade a resident strain, V_1, if the single strain equilibrium

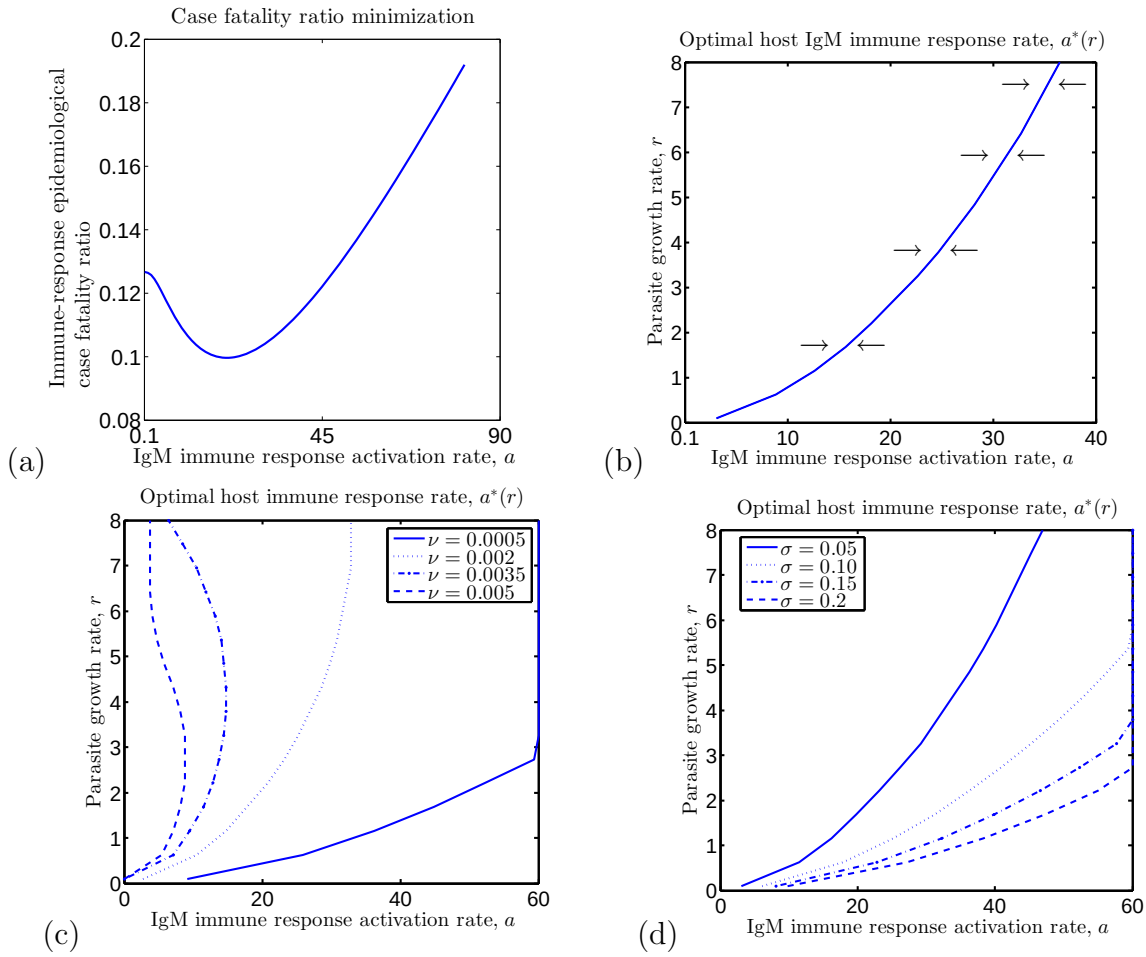

FIGURE 3. *Host evolution, with trait a, with respect to immune response cost and costly pathogen (a) CFR minimization at an intermediate a. (b) The optimality curve, $a^*(r)$, of host immune response rate w.r.t. r. Arrows indicate that every point on $r^*(a)$ is an evolutionary stable strategy (ESS). Here the cost coefficients are fixed at $\sigma = 0.1$ and $\nu = 0.0009$. c) Optimality curve, $a^*(r)$ for increasing values of the parasite damage coefficient σ and for increasing values of immune response cost coefficient ν.*(d)

$\mathcal{E}_1$ is unstable, and once established, V_2 can defend against other strains if $\mathcal{E}_2$ is (locally) asymptotically stable. The conventional wisdom is that a strain with maximal $\mathcal{R}_0$ can both invade and defend against any other strain, and therefore the pathogen evolves toward maximizing $\mathcal{R}_0$. The following theorem indeed establishes $\mathcal{R}_0$ maximization (locally) for the *structured vector-host system with logistic host growth.*

Theorem 3.1. *If $\mathcal{R}_0^1 < \mathcal{R}_0^2$, then the single strain equilibrium $\mathcal{E}_1$ is unstable, i.e. strain-2 invades the resident strain-1 equilibrium. Alternatively, if $\mathcal{R}_0^1 > \mathcal{R}_0^2$ and condition (2.5) holds, then $\mathcal{E}_1$ is locally asymptotically stable.*

(The proof of Theorem 3.1 is in Appendix.)

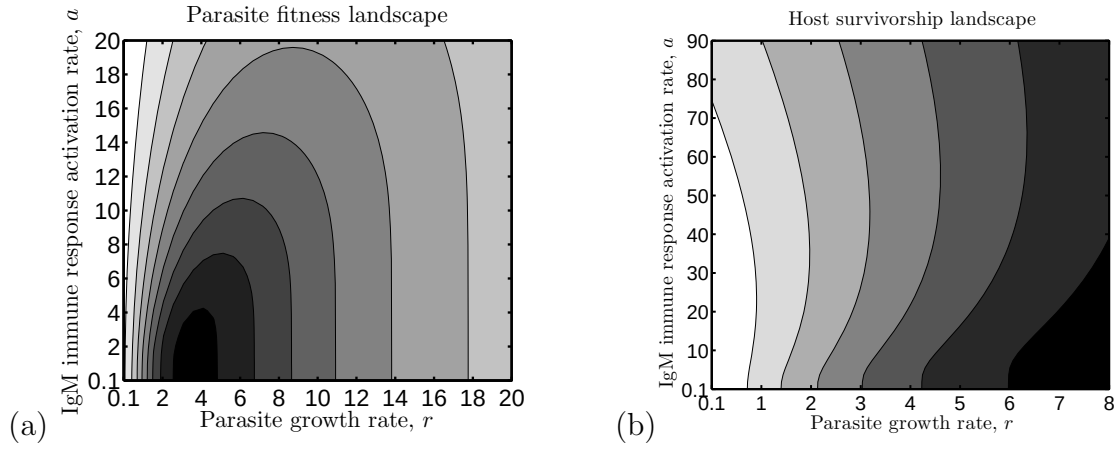

FIGURE 4. a) Parasite fitness landscape across distinct immune activation rate a and parasite growth rate r. b) Host fitness landscape w.r.t. a and r.

Given the assumptions (2.5), Theorem 3.1 suggests that among strains with distinct parasite growth rates, r, the one with largest reproduction number outcompetes the other strains. The value of $r^*(a)$ is the rate r at which reproduction number is maximized with host immune activation rate a (Fig.2a). It represents the optimal balance between parasite mediated and immune response mediated host mortality.

We observe that the optimal parasite replication rate $r^*(a)$ is a monotonically increasing function of a (Fig.2b). When the immune response is smaller, the optimal parasite replication rate gets smaller and may result in larger parasite fitness ($\mathcal{R}_0$) (Fig.4a).

We also perceive that the optimal parasite replication curve $r^*(a)$ is shallower for more damaging parasites (Fig.2c), while it is steeper for more costly immune response (Fig.2d). The parasite optimality curve, $r^*(a)$, increases more drastically and monotonically when parasite damage coefficient σ is smaller or when immune response cost coefficient ν is larger. Thus larger immune response and more damaging immune system favor the evolution of larger parasite replication rates. In contrast, more damaging parasites favor the evolution of lower parasite replication rates.

Compare to the study [17], here we consider a different mode of infection transmission and a within-host model describing arbovirus parasite-host immune response antibody interactions. The numerical and analytical observations in this study shows that the vector-borne pathogen might follow the same evolutionary trajectory with directly transmitted parasites. However, we show in Section 3.3 that vector inoculum size affects the evolution of the pathogen and its virulence, which is a distinctive feature of vector-borne systems. Also, in response to pathogen evolution, host evolution changes the co-evolutionary trajectory resulting in different co-evolutionarily evolutionary stable strategy (Co-ESS).

3.2. **Host Evolution: Case-Fatality Minimization.** Similar to pathogen adaptation, the host also evolves in response to the endemic disease. The pathogen exerts pressure on the host population, so that optimal host immune response properties are evolutionarily favored. Here we consider two host populations differing only in their immune response against the endemic pathogen which is transmitted by the intermediate

vector population:

$$
\begin{cases}
\dfrac{dS_j}{dt} &= \tilde{b}N_j(1-\dfrac{N}{K}) - \beta_1 S_j(t) I_V(t) - dS_j(t) \\
\dfrac{\partial i_j}{\partial t} + \dfrac{\partial i_j}{\partial \tau} &= -(\alpha_j(\tau) + \kappa_j(\tau) + \gamma_j(\tau) + d) i_j(\tau, t), \\
i_j(0,t) &= \beta_1 S_j(t) I_V(t), \\
\dfrac{dR_j}{dt} &= \displaystyle\int_0^\infty \gamma_i(\tau) i_j(\tau, t) d\tau - dR_j(t), \\
\dfrac{dS_V}{dt} &= \eta - S_V(t) \displaystyle\sum_{j=1}^{2} \int_0^\infty \beta_{H_j}(\tau) i_j(\tau, t) d\tau - \mu S_V(t), \\
\dfrac{dI_V}{dt} &= S_V(t) \displaystyle\sum_{j=1}^{2} \int_0^\infty \beta_{H_j}(\tau) i_j(\tau, t) d\tau - \mu I_V(t),
\end{cases}
\tag{3.2}
$$

where $N_j = (S_j + I_j + R_j)$ with $I_j = \displaystyle\int_0^\infty i_j(\tau, t) d\tau$ and $N = N_1 + N_2$. Thus we assume the host populations, $N_j = S_j + \displaystyle\int_0^\infty i_j(\tau, t) d\tau + R_i j$, $j = 1, 2$, have distinct immune parameters, leading to different infectivity, disease-induced mortality and recovery rates, namely $\beta_j(\tau)$, $\nu_j(\tau)$ and $\gamma_j(\tau)$, respectively. The host evolutionary criterium will be based on the case fatality ratio of the host type j, defined as

$$
\mathcal{F}_j = \int_0^\infty \nu_j(\tau) e^{-\int_0^\tau (\nu_j(s) + \gamma_j(s) + d) ds} d\tau,
$$

for $j = 1, 2$. Our main result of this subsection is that hosts evolve toward minimizing the case fatality ratio, $\mathcal{F}$, under selective pressure from the endemic vector-borne pathogen. Prior works have investigated host evolutionary principles for directly transmitted pathogens, however host evolution has not been considered for vector transmitted pathogens. Here we find that minimization of CFR extends to vector-host models with recovered state.

The existence of single host type j endemic equilibria is equivalent to existence of the endemic equilibrium $\mathcal{E}$ in the underlying single host model. Indeed, if the reproduction number for host type j is greater than one; i.e. $\mathcal{R}_j > 1$, then two-host one-strain model (3.2) has a unique host type j equilibrium $\mathcal{E}_j$, where $\mathcal{E}_R = (S_1^*, i_1^*(\tau), R_1^*, 0, 0, 0, S_V^*, I_V^*)$ and $\mathcal{E}_M = (0, 0, 0, S_2^*, i_2^*(\tau), R_2^*, S_V^*, I_V^*)$.

The following theorem establishes the principle of host evolution in response to the vector-borne pathogen, in particular the host with minimum case fatality ratio $\mathcal{F}_j$ invades a resident host population and can stave off invasion from a rare mutant invader.

Theorem 3.2. *If $\mathcal{F}_2 < \mathcal{F}_1$, then the mutant free equilibrium $\mathcal{E}_R = (S_1^*, i_1^*(\tau), R_1^*, 0, 0, 0, S_V^*, I_V^*)$ is unstable i.e. the mutant host population invades the resident host population (local invasion). Otherwise if $\mathcal{F}_1 < \mathcal{F}_2$ and condition (2.5) holds for the resident host, then $\mathcal{E}_R$ is locally asymptotically stable in the two-host one-strain system.*

Proof. Let $(x_1(t), y_1(\tau, t), z_1(t), x_2(t), y_2(\tau, t), z_2(t), u(t), v(t))$ be the small perturbations around the mutant free equilibrium $\mathcal{E}_R$. Linearizing the system (3.2) (with two host-one

strain population) at the mutant free equilibrium $\mathcal{E}_R$, we get:

(3.3)
$$\begin{cases} \lambda x_1 & = -\tilde{b}(\frac{\eta_1+\eta_2}{K})N_1^* + \tilde{b}(1-\frac{N_1^*}{K})\eta_1 - \beta_1(x_1 I_V^* + S_1^* v) - dx_1, \\ \lambda y_1 + \dfrac{dy_1}{d\tau} & = -\left(\gamma_1(\tau)+\alpha_1(\tau)+\kappa_1(\tau)+d\right) y_1(\tau), \\ y_1(0) & = \beta_1(x_1 I_V^* + S_1^* v) \\ \lambda z_1 & = \displaystyle\int_0^\infty \gamma_1(\tau) y_1(\tau) d\tau - dz_1 \\ \lambda u & = -\displaystyle\int_0^\infty \beta_{H_1}(\tau)(u i_1^*(\tau) + S_V^* y_1(\tau)) d\tau - \int_0^\infty \beta_{H_2}(\tau) S_V^* y_2(\tau) d\tau - \mu u, \\ \lambda v & = \displaystyle\int_0^\infty \beta_{H_1}(\tau)(u i_1^*(\tau) + S_V^* y_1(\tau)) d\tau + \int_0^\infty \beta_{H_2}(\tau) S_V^* y_2(\tau) d\tau - \mu v, \\ \lambda x_2 & = \tilde{b}(1-\frac{N_1^*}{K})\eta_2 - \beta_1 x_2 I_V^* - dx_2, \\ \lambda y_2 + \dfrac{dy_2}{d\tau} & = -\left(\gamma_2(\tau)+\alpha_2(\tau)+\kappa_2(\tau)+d\right) y_2(\tau), \\ y_2(0) & = \beta_1 x_2 I_V^*. \\ \lambda z_2 & = \displaystyle\int_0^\infty \gamma_2(\tau) y_2(\tau) d\tau - dz_2, \end{cases}$$

where $\eta_j = x_j + \displaystyle\int_0^\infty y_j(\tau)d\tau + z_j$.

Solving the differential equations, we obtain

(3.4)
$$y_1(\tau) = \beta_1(x_1 I_V^* + S_1^* v) e^{-\lambda\tau}\pi_{H_1(\tau)}, \text{ where } \pi_{H_1}(\tau) = e^{-\displaystyle\int_0^\tau (\gamma_1(s)+\alpha_1(s)+\kappa_1(s)+d)ds}$$

and

(3.5)
$$y_2(\tau) = \beta_1 x_2 I_V^* e^{-\lambda\tau}\pi_{H_2(\tau)}, \text{ where } \pi_{H_2}(\tau) = e^{-\displaystyle\int_0^\tau (\gamma_2(s)+\alpha_2(s)+\kappa_2(s)+d)ds}$$

Note that, any eigenvalue of the system (3.3) is also an eigenvalue of the following decoupled subsystem

(3.6)
$$\begin{cases} \lambda x_2 & = b(1-\frac{N_1^*}{K})n_2 - \beta_1 x_2 I_V^* - dx_2, \\ \lambda y_2 + \dfrac{dy_2(\tau)}{d\tau} & = -\left(\gamma_2(\tau)+\alpha_2(\tau)+\kappa_2(\tau)+d\right) y_2(\tau), \\ y_2(0) & = \beta_1 x_2 I_V^*. \\ \lambda z_2 & = \displaystyle\int_0^\infty \gamma_2(\tau) y_2(\tau) d\tau - dz_2. \end{cases}$$

Rearranging the first equation in (3.6) and substituting $\displaystyle\int_0^\infty y_2(\tau)d\tau$ and $z_2 = \frac{1}{d}\displaystyle\int_0^\infty \gamma_2(\tau)y_2(\tau)d\tau$, we obtain

(3.7)
$$(\lambda - \tilde{b}(1-\frac{N_1^*}{K}) + d + \beta_1 I_V^*)x_2 = \tilde{b}(1-\frac{N_1^*}{K})\int_0^\infty (1+\frac{\gamma_2(\tau)}{\lambda+d})y_2(\tau)d\tau$$

Substituting the equation (3.5) into (3.7), we get

$$(\lambda - \tilde{b}(1 - \frac{N_1^*}{K}) + d + \beta_1 I_V^*) = \tilde{b}(1 - \frac{N_1^*}{K})\beta_1 I_V^*(\int_0^\infty (1 + \frac{\gamma_2(\tau)}{\lambda + d})e^{-\lambda\tau}\pi_{H_2(\tau)d\tau}) \tag{3.8}$$

(assuming $x_2 \neq 0$). Susceptible host type 1 when at equilibrium satisfy

$$\tilde{b}N_1^*(1 - \frac{N_1^*}{K}) - \beta_1 S_1^* I_V^* - dS_V^* = 0 \tag{3.9}$$

where $N_1^* = S_1^* + i_1^*(0)\int_0^\infty \pi_{H_1}(\tau)d\tau + i_1^*(0)\int_0^\infty \frac{\gamma_1(\tau)}{d}\pi_{H_1}(\tau)d\tau$.

$$-\tilde{b}(1 - \frac{N_1^*}{K}) + \beta_1 I_V^* + d = \frac{\tilde{b}(1 - \frac{N_1^*}{K})}{S_1^*}\int_0^\infty (1 + \frac{\gamma_1(\tau)}{d})i_1^*(0)\pi_{H_1}(\tau)d\tau. \tag{3.10}$$

Substituting the right hand side of the equation into (3.8), we obtain the characteristic equation

(3.11)
$$(\lambda + \frac{\tilde{b}(1 - \frac{N_1^*}{K})}{S_1^*}\int_0^\infty (1 + \frac{\gamma_1(\tau)}{d})i_1^*(0)\pi_{H_1}(\tau)d\tau) = \tilde{b}(1 - \frac{N_1^*}{K})\beta_1 I_V^*(\int_0^\infty (1 + \frac{\gamma_2(\tau)}{\lambda + d})e^{-\lambda\tau}\pi_{H_2}(\tau)d\tau)$$

Claim 3.1. *Assume that $\mathcal{F}_1 < \mathcal{F}_2$. Then all eigenvalues of the system (3.3) have negative real part.*

Proof. By the way of contradiction, suppose that the system (3.3) has an eigenvalue λ with nonnegative real part. Then λ also is an eigenvalue of the decoupled subsystem (3.6). Then

(3.12)
$$\left|\lambda + \frac{\tilde{b}(1 - \frac{N_1^*}{K})}{S_1^*}\int_0^\infty (1 + \frac{\gamma_1(\tau)}{d})i_1^*(0)\pi_{H_1}(\tau)d\tau\right| \geq \frac{\tilde{b}(1 - \frac{N_1^*}{K})}{S_1^*}\int_0^\infty (1 + \frac{\gamma_1(\tau)}{d})i_1^*(0)\pi_{H_1}(\tau)d\tau$$

Also for the right hand side of the equation (3.11), we get

(3.13)
$$\left|\tilde{b}(1 - \frac{N_1^*}{K})\beta_1 I_V^*(\int_0^\infty (1 + \frac{\gamma_2(\tau)}{\lambda + d})e^{-\lambda\tau}\pi_{H_2}(\tau)d\tau)\right| \leq \tilde{b}(1 - \frac{N_1^*}{K})\beta_1 I_V^*(\int_0^\infty (1 + \frac{\gamma_2(\tau)}{d})\pi_{H_2}(\tau)d\tau).$$

Then by (3.12) and (3.13) if

(3.14)
$$\int_0^\infty (1 + \frac{\gamma_1(\tau)}{d})i_1^*(0)\pi_{H_1}(\tau)d\tau \leq \beta_1 I_V^* S_1^*(\int_0^\infty (1 + \frac{\gamma_2(\tau)}{d})\pi_{H_2(\tau)d\tau}), \text{ where } i_1^*(0) = \beta_1 I_V^* S_1^*.$$

Therefore,

$$\int_0^\infty (\frac{d + \gamma_1(\tau)}{d})\pi_{H_1}(\tau)d\tau \leq \int_0^\infty (\frac{d + \gamma_2(\tau)}{d})\pi_{H_2}(\tau)d\tau. \tag{3.15}$$

Subtracting and adding $\nu_1(\tau)$ on the left hand side of the equation above and $\nu_2(\tau)$ on the right side of the equation, we obtain

$$1 - \int_0^\infty \nu_1(\tau)\pi_{H_1}(\tau)d\tau \leq 1 - \int_0^\infty \nu_2(\tau)\pi_{H_2}(\tau)d\tau.$$

Then

$$\int_0^\infty \nu_1(\tau)\pi_{H_1}(\tau)d\tau \geq \int_0^\infty \nu_2(\tau)\pi_{H_2}(\tau)d\tau,$$

which implies that $\mathcal{F}_1 \geq \mathcal{F}_2$. It is a contradiction. This completes the proof for the case $x_2 \neq 0$. Now assume that $x_2 = 0$. Then $\eta_2 = 0$, in which case we obtain the subsystem

$$\begin{cases} \lambda x_1 & = -\tilde{b}(\frac{\eta_1 N_1^*}{K}) + \tilde{b}(1 - \frac{N_1^*}{K})\eta_1 - \beta_1(x_1 I_V^* + S_1^* v) - dx_1, \\ \lambda y_1(\tau) + \frac{dy_1(\tau)}{d\tau} & = -\left(\gamma_1(\tau) + \alpha_1(\tau) + \kappa_1(\tau) + d\right) y_1(\tau), \\ y_1(0) & = \beta_1(x_1 I_V^* + S_1^* v) \\ \lambda z_1 & = \int_0^\infty \gamma_1(\tau) y_1(\tau)d\tau - dz_1 \\ \lambda u & = -\int_0^\infty \beta_{H_1}(\tau)(u i_1^*(\tau) + S_V^* y_1(\tau))d\tau - \mu u, \\ \lambda v & = \int_0^\infty \beta_{H_1}(\tau)(u i_1^*(\tau) + S_V^* y_1(\tau))d\tau - \mu v. \end{cases} \tag{3.16}$$

This is exactly the linearized system determining the local stability of $\mathcal{E}$, the endemic equilibrium for the single-host single-strain model. Thus, by Theorem 2.1, the conditions (2.5) imply that the eigenvalues of subsystem (3.16) have negative real part. Then the case $x_2 = 0$ also contradicts the assumption that the system (3.3) has an eigenvalue with nonnegative real part. □

Then, when $\mathcal{F}_1 < \mathcal{F}_2$ and boundary conditions hold, the mutant free equilibrium is locally asymptotically stable.

Claim 3.2. *(Local invasion) If $\mathcal{F}_2 < \mathcal{F}_1$. Then the mutant free equilibrium $\mathcal{E}_R^*$ is unstable; i.e. mutant population invades resident population.*

Proof. Let define the left hand-side of the equation (3.11) as $g(\lambda)$ and the right hand-side as $f(\lambda)$. Note that any λ solution of this system must be an eigenvalue of the decoupled subsystem (3.16). Now we want to show that the equation (3.11) has a positive real root λ, whenever $\mathcal{F}_2 < \mathcal{F}_1$. First note that $g(\lambda)$ is an increasing function of λ and $f(\lambda)$ is a decreasing function of λ for $\lambda \in \mathbb{R}$. Therefore, if $g(0) < f(0)$, then the equality (3.11) has a positive real root λ. Next we want to show that $g(0) < f(0) \Leftrightarrow \mathcal{F}_2 < \mathcal{F}_1$. Note that

$$g(0) < f(0)$$
$$\Leftrightarrow$$
$$\int_0^\infty (1 + \frac{\gamma_1(\tau)}{d}) i_1^*(0)\pi_{H_1}(\tau)d\tau < \beta_1 I_V^* S_1^* (\int_0^\infty (1 + \frac{\gamma_2(\tau)}{d})\pi_{H_2(\tau)d\tau}),$$

where $i_1^*(0) = \beta_1 I_V^* S_1^*$. Then the rest of the proof follows similar steps to the proof of Claim (3.1) after the inequality (3.14). □

□

Remark 3.1. *Condition (2.5) can be replaced by the more general condition that the resident equilibrium $\mathcal{E}_R$ is locally stable for the single host model (**??**), i.e. locally stable on the boundary. If the resident endemic equilibrium in the one host system is unstable, it is questionable to investigate what happens when mutant arrives at resident equilibrium.*

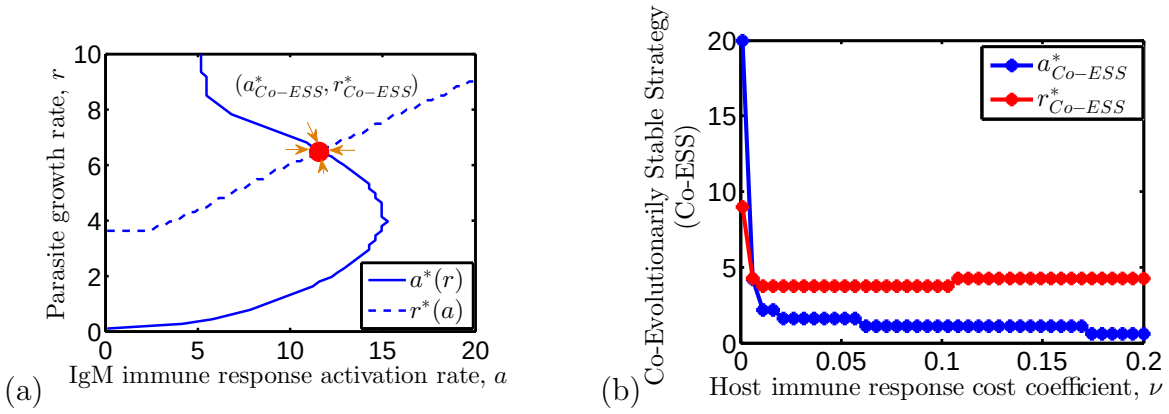

FIGURE 5. a) Evolutionary trajectories of host immune response and parasite growth rate and their Coevolutionary Evolutionarily Stable Strategy (CoESS). b) CoESS vs. varying immune response cost coefficient, ν.

Most likely the instability will be in the form of sustained oscillations in which case the analysis requires to use Floquet Theory (work in progress).

Theorem 3.2 suggests that a rare mutant host population with smaller $\mathcal{F}(a)$ can invade the resident population. By way of adaptive dynamics, we infer that the host population evolves toward minimizing the Case Fatality Ratio, $\mathcal{F}$. Notice that the minimization of CFR is newly observed phenomenon in host evolution. In a very recent study, Martcheva et al. [14] show that in a directly transmitted disease with recovery or chronic stage, host might evolve minimization the case fatality ratio. We see that this result extends to the systems with vector-borne pathogen-host systems.

The Case Fatality Ratio (CFR):

$$\mathcal{F}_j = \int_0^\infty \nu_j(\tau) e^{-\int_0^\tau (\nu_j(s)+\gamma_j(s)+d)ds} d\tau,$$

for $j = 1, 2$. is the ratio of host type-j death due to disease and it is clear that it depends on *pathogen-host immune response* via parameters $\nu_j(\tau), \gamma_j(\tau)$ governing by within-host pathogen-immune response. Assuming the IgG immune response activation rate a is a trait of the host, numerical results suggest that, the unique optimal immune response a^* that minimizes CFR is an intermediate host response a (Fig.3(a)). For larger trade off constants, we also observe that it is sometimes the best for the host not to have any immune response ($a^* = 0$), which is biologically reasonable.

The optimal host immune response $a^*(r)$, is the IgM immune response activation rate a that minimizes the CFR in response to pathogen evolution trait r. We observe that small parasite growth rates,r, reduce the optimal host immune response $a^*(r)$, leading reduction in $\mathcal{F}$ (Fig.3(b)). The biological reasoning is that when the parasite replication rate is small, the larger immune response can only harm the host, leading to death. Thus the optimal host strategy is to have less and effective immune response, when parasite is less invasive.

The optimal immune response rate $a^*(r)$ is a monotonically increasing function of r, given that the immune cost is small. Yet, when damage due to immune response is large, the host optimality curve $a^*(r)$ is a concave down function of r, which suggests that when immune cost is large, host evolution favors smaller immune response in response to large pathogen replication rate r as well (Fig. 3(c)). This suggests that when the immune response becomes more costly (increasing ν), the optimal host strategy evolves toward using less resources toward clearing the parasitic infection. Numerical results also suggest that larger parasite growth and more damaging pathogen (higher σ) favor the evolution of larger immune response rate (Fig.3(d)); in contrast to more damaging host immune response (higher ν) favoring evolution of lower immune response rates.

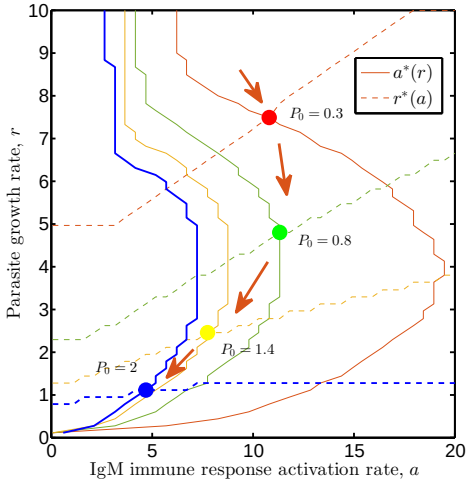

FIGURE 6. The affect of changing vector inoculum size on the evolutionary trajectories of the coevolving host-parasite systems. Increase in the inoculum size decreases coevolutionary attractor $(a^*_{CoESS}, r^*_{CoESS})$.

3.3. **Coevolution of Host-Vector Borne Pathogen.** Host evolution favors minimization of $\mathcal{F}$, and the pathogen population can also evolve toward maximizing $\mathcal{R}_0$. With both processes occuring, the pathogen and host engage in evolutionary arms race. Assuming that this evolutionary process continues until the optimal parasite growth rate and the optimal host immune response rate reach a coevolutionary attractor (a^*, r^*) such that $r^*(a^*) = r^*$ and $a^*(r^*) = a^*$. The intersection of the curves $r^*(a)$ and $a^*(r)$ gives the values for $(a^*_{Co-ESS}, r^*_{Co-ESS})$, where at this pair (coevolutionary evolutionarily stable strategy), host and parasite have the optimal host response, and optimal parasite growth rate, respectively (See Fig.5a).

The coevolutionary trajectory of the whole system is governed by the trajectories of the system $\dot{a} = \frac{\partial \mathcal{F}}{\partial a}, \dot{r} = k\frac{\partial \mathcal{R}_0}{\partial r}$, in the ar plane (similar to [17]) where k is the ratio of the parasite's rate of evolutionary change to its host's rate of evolutionary change. Most likely $k > 1$ since the pathogen turn over rate is higher than the host's, as indicated in [17]. Thus trajectories will more closely follow the optimality curve $r^*(a)$. The coevolutionary attractor $(a^*_{Co-ESS}, r^*_{Co-ESS})$ is the point where both $\frac{\partial \mathcal{F}}{\partial a}|_{a=a^*_{Co-ESS}} = 0$, $\frac{\partial \mathcal{R}_0}{\partial r}|_{r^*_{Co-ESS}} = 0$.

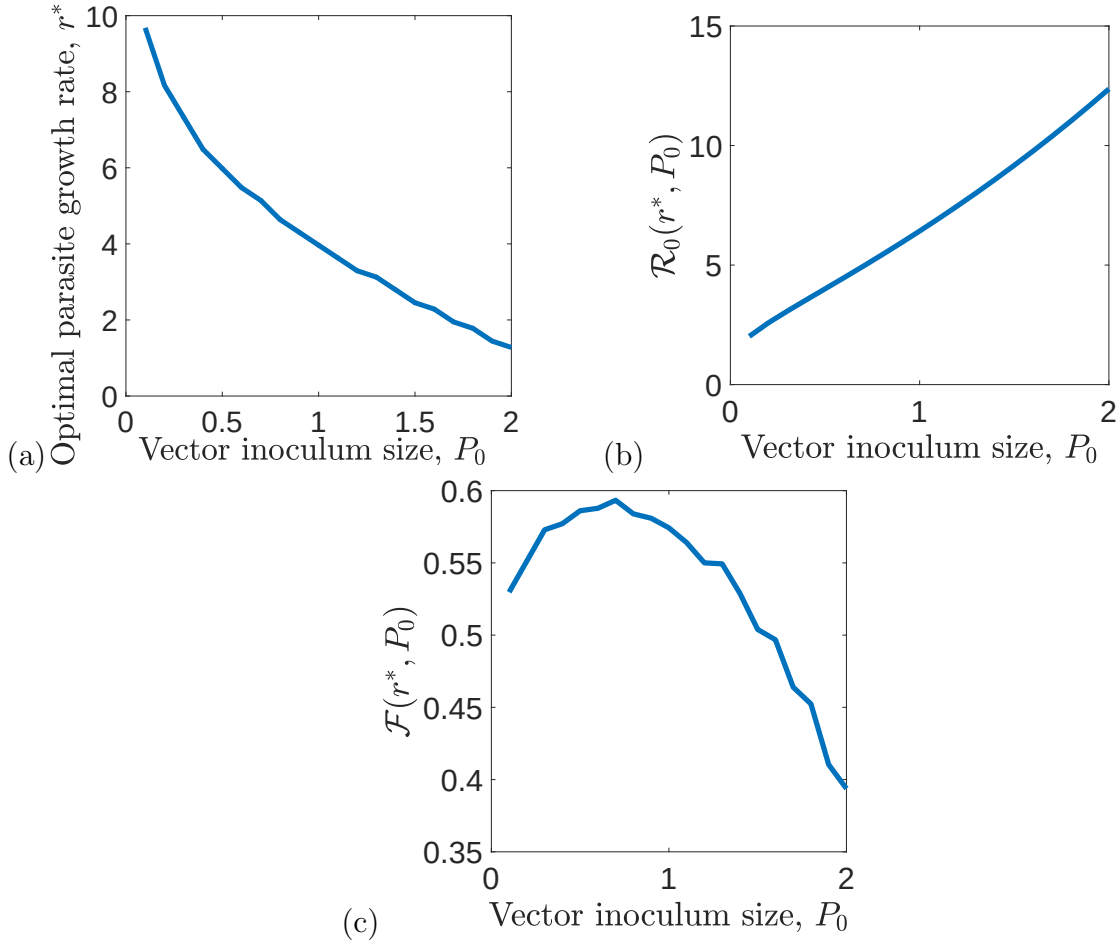

FIGURE 7. a) Optimal parasite growth rate r^* w.r.t. vector inoculum size P_0. b) $\mathcal{R}_0$ w.r.t P_0 and $r^*(P_0)$. c) CFR $\mathcal{F}$ w.r.t. P_0 and $r^*(P_0)$.

Here, we observe that the location of the Co-ESS point $(a^*_{Co_ESS}, r^*_{Co_ESS})$ changes with respect to the cost coefficients σ and ν. The *cost coefficients* σ and ν are the constants weighting the disease induced death rate w.r.t. parasite resource use or aggressive immune response, respectively. For fixed value of σ, for smaller immune cost, a small increase in immune cost coefficient ν decreases the Co-ESS pathogen growth rate r^*_{Co-ESS}; yet for larger immune cost, a small increase in immune cost coefficient increases or stabilizes r^*_{Co-ESS} (Fig.5). However increase in the immune cost always decreases Co-ESS immune response a^*_{Co-ESS}. For large immune cost, immune response evolves toward vanishing.

An interesting outcome is that a pathogen and a host, initially with low virulence and a less active immune response, can be driven toward the more virulent and immune active coevolutionary attractor. We observe that at the CoESS parasite growth and host immune response rate $(a^*_{Co-ESS}, r^*_{Co-ESS})$ in Fig.5(a), the reproduction number $\mathcal{R}_0$ is smaller and $\mathcal{F}$ is larger then initially. For example, in the darkest region in the Fig.4(a), $\mathcal{R}_0$ has the largest value and the Case Fatality Ratio $\mathcal{F}$ is smaller; yet at the coevolutionary attractor $(a^*_{Co-ESS}, r^*_{Co-ESS})$, $\mathcal{F}$ has a larger value and $\mathcal{R}_0$ has a smaller value

(See Fig.9 in Appendix). Thus the nature of virus-host interactions can lead the system to evolve toward a less favorable outcome for both pathogen and host. Indeed, for both directly transmitted and vector transmitted, the antagonism of virus and host can lead to this result where the coevolutionary attractor is "less optimal" for both populations.

The vector transmitted parasite inoculum, defined by (average) initial pathogen concentration P_0, does affect the coevolutionary attractor, and provides a distinction from nested models with direct transmission. A previous study [50] suggests that evolution to higher virulences for vector-borne pathogens might be caused by larger initial inoculum sizes that vectors inject into hosts. The vector transmitted inoculum is likely to be independent of the pathogen load of the host infector, as opposed to direct transmission, thereby fitting the assumptions of the nested model and providing a particularly nice parameter to study its affect on coevolution. Therefore we vary vector parasite inoculum and investigate its influence on the coevolutionary attractor. There are multiple theories on how the vector-borne pathogen may affect the vector[53, 54, 55, 56, 51], but here we do not impose any costs to vectors carrying the virus. We numerically observe that increase in vector inoculum reduces a and r in the coevolutionary attractor (See Fig.6(a)).

How CFR and $\mathcal{R}_0$ at the Co-ESS immune response and parasite growth rate scales across different inoculum size is an important question. Mathematically, the CFR, $\mathcal{F}(a^*_{CoESS}, r^*_{CoESS}, P_0)$, and the reproduction number, $\mathcal{R}_0(a^*_{CoESS}, r^*_{CoESS}, P_0)$, are highly nonlinear functions of Co-ESS immune response and parasite growth rate $(a^*_{CoESS}, r^*_{CoESS}, P_0)$, and these coevolutionary attractors are also highly nonlinear functions of the optimal ESS, $(a^*(P_0), r^*(P_0))$, where at fixed inoculum size P_0, a^* is the optimal host immune activation rate minimizing the CFR and r^* maximizes the pathogen reproduction number.

Our numerical results suggest that inoculum size changes $(a^*_{Co-ESS}, r^*_{Co-ESS})$ significantly. The Fig.8(a) shows the CoESS attractors, $(a^*_{Co-ESS}, r^*_{Co-ESS})$, w.r.t. vector inoculum size P_0 and the Fig.8(a) displays how CFR and $\mathcal{R}_0$ change at these range of P_0. In part (b), we observe that there are multiple critical vector inoculum sizes, namely $P_0^{c_1}$ and $P_0^{c_2}$, such that between these two critical points, an increase in inoculum size results in lower CFR. Otherwise when $P_0 < P_0^{c_1}$, or $P_0 > P_0^{c_2}$, it results in higher CFR. There might be more critical inoculum size points as P_0 increases further, but there should also be a physiological limit to vector inoculum size. Our results show that larger inoculums transmitted by vectors can result in higher virulence up to a point $(P_0 \leq P_0^{c_1})$, which lends support to the claim in [] that higher virulences observed in vector-borne diseases may be due to larger inoculum size. However, further increase in P_0 substantially decreases host CFR, which might be a favorable outcome for the vector population since vectors feed on the host population. Thus it may be the case that evolution drives vectors toward being more and more efficient in carrying and injecting the pathogen, resulting in less virulence.

In the absence of host evolution, the Figure 7(a) shows that the optimal growth rate, r^*, decreases as vector inoculum size P_0 increases. Yet, the parasite reproductive fitness

$\mathcal{R}_0(r^*, P_0)$ increases (Fig. 7(b)). The CFR $\mathcal{F}(r^*, P_0)$ is non-monotone function of P_0, as similar to at CoESS parasite growth and host immune response rates (Fig. 7(c)). These results suggest that pathogen evolution might be a more driving force on the co-evolution of both host and parasites.

We remark that the birth and death parameters along with vector to host transmission rate, β_1, do not influence the coevolutionary pathogen-host attractor $(a^*_{Co-ESS}, r^*_{Co-ESS})$. One way to see this is by looking at the $\mathcal{R}_0$ formula, where the optimal replication rate r^* does not change with vector growth or death rate. However, these parameters may influence abundance of vectors, which can play a crucial role on disease persistence and prevalence.

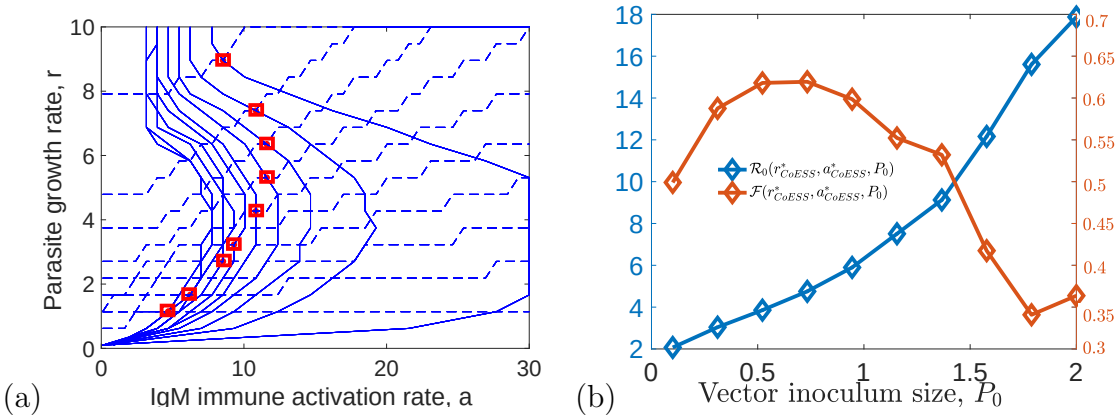

FIGURE 8. Host Case Fatality Ratio $\mathcal{F}$ and Parasite Reproduction number $\mathcal{R}_0$ v.s. inoculum size P_0. a) $(a^*_{CoESS}, r^*_{CoESS})$ w.r.t. vector inoculum size P_0. b) $\mathcal{R}_0$ and $\mathcal{F}$ w.r.t. $((a^*_{CoESS}, r^*_{CoESS}), P_0)$.

4. Discussion

Highly dynamic host and parasite interactions give rise to their evolution. Parasite fitness is determined by its ability to infect and multiply within a host while it must leave its current host and become transmitted to the next host individual. However, the actions of the parasite may harm the host – either directly or as a consequences of the host's defense reactions. In both cases, the parasite becomes virulent to its host. On the other hand, hosts defend themselves against infection through an immune response, leading to coevolution of parasites and hosts. Here, we particularly study evolution of host and vector-borne pathogens.

Our analytical results suggest that host evolution tends to minimize the case fatality ratio (CFR): $\mathcal{F} = \int_0^\infty \nu(\tau) e^{-\int_0^\tau (\nu(s)+\gamma(s)+d)ds} d\tau$, where the epidemiological parameter functions ν and γ are governed by pathogen and immune response antibody dynamics. Considering immune response activation rate a as a host trait, we numerically and analytically found that hosts evolution trait a evolve toward an intermediate value. We obtain that the host response optimality curve $a^*(r)$ is a monotonically increasing function of r when immune cost is small. Yet, when immune response is too costly, the optimal host strategy evolves toward using less resources to clear the parasitic infection,

even when r is large. When the parasite growth rate,r, is smaller, the optimal host immune response $a^*(r)$ becomes smaller resulting in smaller $\mathcal{F}$ and smaller $\mathcal{R}_0$, which is a better outcome for the host population. We find that the pathogen evolves towards maximizing its reproduction number, $\mathcal{R}_0$, agreeing with previous studies. The parasite replication optimality curve $r^*(a) = \underset{r}{\operatorname{argmax}}\, \mathcal{R}_0$ is also an increasing monotone function of host trait a. When the immune response is smaller, the optimal parasite replication rate gets smaller, resulting in larger parasite fitness ($\mathcal{R}_0$) and less host mortality (smaller $\mathcal{F}$) (better outcome for both host and parasite).

The characterization of the coevolutionary attractor $(a_{Co\_ESS}, r_{Co\_ESS}) = (a, r) : r^*(a) = a^*(r)$ for this system is a computationally difficult question. By using a numerical scheme, we observe that in vector-borne systems, the coevolutionary dynamics can result in trajectories which moves toward decreased values of $\mathcal{R}_0$ and increased values of $\mathcal{F}$ (an inferior outcome for both pathogen and host). Interestingly, we observe that vector inoculum size, P_0, has significant affect on the coevolutionary attractor of host and vector-borne pathogens. While the $\mathcal{R}_0$ observed at the coevolutionary attractor always increases as P_0 increases, the evolution of the CFR, $\mathcal{F}$, has a more complex relationship with P_0. Increasing P_0 causes an evolutionary attractor with higher CFR (virulence) up to a critical value of P_0, which may support the hypothesis in [] that vector-borne diseases can evolve higher virulence due to larger inoculum sizes injected in the hosts. However, increasing vector inoculum size larger than this critical value results in a CoESS host immune response and pathogen growth rate $(a^*_{Co-ESS}, r^*_{Co-ESS})$ that reduces CFR, which is beneficial to host and may be favorable for vector population also. We also demonstrate that vector birth and death rates do not affect the coevolutionary attractor, despite the fact that these parameters play a crucial role on disease persistence. Further studies in more biologically detailed vector-borne pathogen-host models may delineate the effects of vector parameters on vector-borne pathogen-host evolution.

More readily available within-host data motivates us to development of better immuno-epidemiological models in order to potentially predict the impact of control strategies such as vaccination or treatment [59, 66, 67]. Future work will also address both impact of vaccination in immuno-epidemiological parasite-host systems and further computation of evolutionary stable strategies (ESS), especially for cases when the resident population is undergoing sustained oscillations.

5. Acknowledgment

The authors H. Gulbudak and V. Cannataro acknowledge partial support from IGERT grant NSF DGE-0801544 in the Quantitative Spatial Ecology, Evolution and Environment Program at the University of Florida. Authors N. Tuncer and M. Martcheva would also like to acknowledge support from the National Science Foundation (NSF) under grants DMS-1515661/DMS-1515442.

References

[1] Tuncer, N. and Gulbudak, H. and Cannataro, V. L. and Martcheva, M., Structural and Practical Identifiability Issues of Immuno-Epidemiological Vector–Host Models with Application to Rift Valley Fever. *Bulletin of Mathematical Biology* **78(9)** (2016), p.1796–1827.

[2] M. Pepin, M. Bouloy, B.H. Bird, A. Kemp, J. Paweska, Rift Valley fever virus (Bunyaviridae: Phlebovirus): an update on pathogenesis, molecular epidemiology, vectors, diagnostics and prevention. *Veterinary Research* **41** (2010), p. 61

[3] B.H. Bird, T.G. Ksiazek, S.T. Nichol, N.J. Maclachlan, Rift Valley fever virus, *J. Am. Vet. Med. Assoc.* **234** (2009), p. 883-893.

[4] R. Ben-Shachar, K. Koelle, Minimal within-host dengue models highlight the specific roles of the immune response in primary and secondary dengue infections *J. R. Soc. Interface* **12 (103)** (2015), 20140886.

[5] Viral Load, Wikipedia, https://en.wikipedia.org/wiki/Viral_load (accessed 12/17/2015).

[6] Dengue and severe dengue, WHO, http://www.who.int/mediacentre/factsheets/fs117/en/ (accessed 12/19/2015).

[7] J. Paweska, F. Burt, F. Anthony, S. Smith, A. Grobbelaar, J. Croft, T. Ksiazek, R. Swanepoel IgG-sandwich and IgM-capture enzyme-linked immunosorbent assay for the detection of antibody to Rift Valley fever virus in domestic ruminants. *Journal of Virological Methods* **113** (2003), p. 103-112.

[8] J. Morrill, F. Knauert, T. Ksiazek Rift Valley fever infection of rhesus monkeys: implications for rapid diagnosis of human disease. *Research in Virology* **140** (1989) p.139-146.

[9] R. Nikin-Beers, S. M. Ciupe, The role of antibody in enhancing dengue virus infection, *Mathematical Biosciences* **263** (2015), p. 83-92.

[10] Fraser et al., Virulence and pathogenesis of HIV-1 infection: an evolutionary perspective, [**?**] **343** (2014), 1243727 (doi:10.1126/science.1243727).

[11] A. Handel, P. Rohani, Crossing the scale from within-host infection dynamics to transmission fitness: A discussion of current assumptions and knowledge, *Philosophical Transactions of the Royal Society of London B***370** (2015), p. 20140302

[12] B. Hellriegel, Immunoepidemiology bridging the gap between immunology and epidemiology, *TRENDS in Parasitology* **17** (2001), p.102-106.

[13] Day, Troy and Proulx, Stephen R. , A general theory for the evolutionary dynamics of virulence,*The American Naturalist* **163(4)** (2004), p. E40–E63.

[14] Martcheva, Maia and Tuncer, Necibe and Kim, Yena, On the principle of host evolution in host–pathogen interactions,*Journal of biological dynamics* (2016), p.1–18.

[15] A. Pugliese, The role of host population heterogeneity in the evolution of virulence, *Journal of biological dynamics* **5 (2)** (2011), p. 104-119.

[16] Woolhouse, Mark E J and Webster, Joanne P and Domingo, Esteban and Charlesworth, Brian and Levin, Bruce R, Biological and biomedical implications of the co-evolution of pathogens and their hosts. *Nature genetics* **32** (2002), p. 569–577.

[17] M. A. Gilchrist, A. Sasaki, Modeling host-parasite coevolution: a nested approach based on mechanistic models,*Journal of Theoretical Biology* **218** (2002), p. 289-308.

[18] M.A. Gilchrist, D. Coombs, The evolution of virulence: interdependence, constraints and selection using nested models, *Theoretical Population Biology* **69** (2006), p. 145-153.

[19] J.B. André, J.B. Ferdy, B. Godelle, Within-host parasite dynamics, emerging tradeoff, and evolution of virulence with immune system. *Evolution* **57** (2003), p. 1489-1497.

[20] B. Boldin, O. Diekmann, Superinfections can induce evolutionarily stable coexistence of pathogens, *Journal of Mathematical Biology***56 (5)** (2008), p. 635-672.

[21] R. M. Anderson, R. M. May, Coevolution of Hosts and Parasites, *Parasitology* **85** (1982), p. 411-426.

[22] B. Alberts, A. Johnson, J. Lewis, M. Raff, K. Roberts, P. Walter, Molecular Biology of the Cell, 4th edition, Garland Science, New York, 2002, Chapter 25.

[23] S. Alizon, M. Van Baalen, Emergence of a convex trade-off between transmission and virulence. *The American naturalist.* **165** (2005), p. E155-167.

[24] H. G. BREMERMANN, H. R. THIEME, A competitive exclusion princible for pathogen virulence, *Journal of Mathematical Biology***27** (1989) p. 179-190.
[25] L. M. CAI, M. MARTCHEVA, X. Z. LI, Competitive exclusion in a vector-host epidemic model with distributed delay(), *Journal of Biological Dynamics* **7** (2013), p. 47-67.
[26] ZHAO, XIAO-QIANG, Dynamical systems in population biology, *Springer Science & Business Media* (2013)
[27] J.Y. YANG, X.Z.LI, M. MARTCHEVA, Global Stability of a DS-DI Epidemic Model with Age of Infection, *J. Math. Anal. Appl.***385** (2012), p. 655-671.
[28] M. MARTCHEVA, X. Z. LI, Linking immunological and epidemiological dynamics of HIV: The case of super-infection, *J. Biol. Dyn. Vol.* **7 (1)** (2013), p. 161-182.
[29] J.Y. YANG, X.Z.LI, M. MARTCHEVA, Global Stability of a DS-DI Epidemic Model with Age of Infection, *J. Math. Anal. Appl.***385** (2012), p. 655-671.
[30] FENG, Z. AND VELASCO-HERNÁNDEZ, J. X., Competitive exclusion in a vector-host model for the dengue fever, *Journal of mathematical biology***35(5)** (1997), p. 523–544.
[31] K. KOELLE, ET AL., Epochal evolution shapes the phylodynamics of interpandemic influenza A (H3N2) in humans, *Science* **314.5807** (2006), p. 1898-1903.
[32] S. KRYAZHIMSKIY, ET AL., On state-space reduction in multi-strain pathogen models, with an application to antigenic drift in influenza A, *PLoS Comput Biol* **3 (8)** (2007), e159.
[33] HONJO, TASUKU AND KINOSHITA, KAZUO AND MURAMATSU, MASAMICHI, Molecular mechanism of class switch recombination: linkage with somatic hypermutation. *Annual review of immunology* **20** (2002), p. 165–96.
[34] N.M. NGUYEN ET AL., Host and viral features of human dengue cases shape the population of infected and infectious Aedes aegypti mosquitoes, [**?**]**110 (22)** (2013), p.9072-9077 (doi:10.1073/pnas.1303395110)
[35] MACKINNON, M. J. AND READ, A., Selection for high and low virulence in the malaria parasite. *Proceedings of the Royal Society of London B: Biological Sciences* **266 (1420)** (1999), p. 741–748.
[36] DWYER, G. AND LEVIN, S. A. AND BUTTEL, L., A simulation model of the population dynamics and evolution of myxomatosis. *Ecological Monographs* **60 (4)** (1990), p. 423–447.
[37] EWALD, P. W., Host-parasite relations, vectors, and the evolution of disease severity. *Annual Review of Ecology and Systematics* **14** (1983), p. 465–485.
[38] EWALD, P. W., Evolution of infectious disease. *Oxford University Press on Demand* (1994).
[39] BARREIRO, L. B. AND QUINTANA-MURCI, L. ÍS, From evolutionary genetics to human immunology: how selection shapes host defence genes. *Nature Reviews Genetics* **11(1)** (2010), p. 17–30.
[40] GANDON, S. AND VALE, P. F., The evolution of resistance against good and bad infections. *Journal of evolutionary biology* **27(2)** (2014), p. 303–312.
[41] BOWERS, R. G., The basic depression ratio of the host: the evolution of host resistance to microparasites. *Proceedings of the Royal Society of London B: Biological Sciences* **268(1464)** (2001), p. 243–250.
[42] BOOTS, M. AND HARAGUCHI, Y., The evolution of costly resistance in host-parasite systems. *The American Naturalist* **153(4)** (1999), p.359–370.
[43] GIAFIS, A. AND BOWERS, R. G., The adaptive dynamics of the evolution of host resistance to indirectly transmitted microparasites. *Mathematical biosciences* **210(2)** (2007), p.668–679.
[44] MILLER, M. R., WHITE, A ., AND BOOTS, M., The evolution of host resistance: tolerance and control as distinct strategies. *Journal of theoretical biology* **236(2)** (2005), p.198–207.
[45] P. MAGAL, C. MCCLUSKEY, Two-group infection age model including an application to nosocomial infection, *SIAM Journal on Applied Mathematics***73 (2)** (2013), p.1058-1095.
[46] F. DERCOLE, S. RINALDI, Analysis of Evolutionary Processes: The Adaptive Dynamics Approach and Its Applications, Princeton University Press, Princeton, NJ, 2008.
[47] U. DIECKMANN, J.A.J. METZ, M.W. SABLIS, K. SIGMUND (EDS.), Adaptive Dynamics of Infectious Diseases: In Pursuit of Virulence Management, Cambridge University Press, Cambridge, UK, 2002.
[48] A. GANDOLFI, A. PUGLIESE, C. SINISGALLI, Epidemic dynamics and host immune response: a nested approach, *Journal of Mathematical Biology* **70.3** (2014), p. 399-435.

[49] Cressler, C. E. et al., The adaptive evolution of virulence: a review of theoretical predictions and empirical tests, *Parasitology* **143(07)** (2016), p. 915–930.
[50] Day, Troy The evolution of virulence in vector-borne and directly transmitted parasites, *Theoretical population biology***62(2)** (2002), p.199–213.
[51] Froissart, R. et al. The virulence–transmission trade-off in vector-borne plant viruses: a review of (non-) existing studies, , *Philosophical Transactions of the Royal Society of London B: Biological Sciences***365(1548)** (2010), p.1907–1918.
[52] Alizon, S. and Hurford, A. and Mideo, N. and Van Baalen, M. Virulence evolution and the trade-off hypothesis: history, current state of affairs and the future, *Journal of evolutionary biology***22(2)** (2009), p.245–259.
[53] Elliot, Sam L and Adler, Frederick R and Sabelis, Maurice W How virulent should a parasite be to its vector?, *Ecology***84(10)** (2003), p.2568–2574.
[54] Lambrechts, Louis and Scott, Thomas W Mode of transmission and the evolution of arbovirus virulence in mosquito vectors, *Proceedings of the Royal Society of London B: Biological Sciences* (2009), rspb–2008.
[55] Ciota, Alexander T. et al. The evolution of virulence of West Nile virus in a mosquito vector: implications for arbovirus adaptation and evolution, *BMC evolutionary biology*13(1)(2013), p.1.
[56] Kenney, J and Brault, A The role of environmental, virological and vector interactions in dictating biological transmission of arthropod-borne viruses by mosquitoes, *Adv. Virus Res***89** (2014), p.39–83.
[57] Antia, R. and Levin, B. R. and May, R. M. Within-host population dynamics and the evolution and maintenance of microparasite virulence, *American Naturalist*(1994), p.457–472.
[58] Antia, R. and Lipsitch, M. Mathematical models of parasite responses to host immune defences, *Parasitology***115(07)** (1997), p.155–167.
[59] Ganusov, V. V. and Antia, R. Imperfect vaccines and the evolution of pathogens causing acute infections in vertebrates, *Evolution***60(5)** (2006), p.957–969.
[60] Ganusov, V. V., Bergstrom, C. T., Antia, R. Within-host population dynamics and the evolution of microparasites in a heterogeneous host population, *Evolution* **56(2)** (2002), p.213–223.
[61] Alizon, S. and Luciani, F. and Regoes, R. R. Epidemiological and clinical consequences of within-host evolution, *Trends in microbiology* **19(1)** (2011), p.24–32.
[62] Alizon, S. and Lion, S. Within-host parasite cooperation and the evolution of virulence, *Proceedings of the Royal Society of London B: Biological Sciences*(2011), rspb20110471.
[63] André, J. B. and Gandon, S. Vaccination, within-host dynamics, and virulence evolution, *Evolution* **60(1)** (2006), p.13–23.
[64] Ball, C. L. and Gilchrist, M. A. and Coombs, D. Modeling within-host evolution of HIV: mutation, competition and strain replacement, *Bulletin of mathematical biology* **69(7)** (2007), p.2361–2385.
[65] Coombs, D. and Gilchrist, M. A. and Ball, C. L. Evaluating the importance of within- and between-host selection pressures on the evolution of chronic pathogens, *Theoretical population biology* **72(4)** (2007), p.576–591.
[66] Gulbudak, H. and Martcheva, M. A structured avian influenza model with imperfect vaccination and vaccine-induced asymptomatic infection, *Bulletin of mathematical biology* **76(10)** (2014), p.2389–2425.
[67] Lin, C.-J. and Deger, K. A. and Tien, J. H. Modeling the trade-off between transmissibility and contact in infectious disease dynamics, *Mathematical biosciences* **277** (2016), p.15–24.

6. Appendix

6.1. **Analysis of immunological model: Virus ultimately clears.** Notice that in the system (2.1), in the absence of immune response ($M_0 = 0, G_0 = 0$), the pathogen grows exponentially, in which case it is expected that the infected host dies since the

parasite damages the host. However, when immune system is active, we establish the following result:

Theorem 6.1. *If initial immune response is active ($M_0 > 0$ or $G_0 > 0$), then the pathogen eventually clears ($\lim_{\tau\to\infty} P(\tau) = 0$), the IgM immune response antibodies decays to zero after viral clearance and subsequently the IgG immune memory antibodies reach a steady-state; i.e.* $\lim_{\tau\to\infty} M(\tau) = 0$ *and* $\lim_{\tau\to\infty} G(\tau) = G^*$, *where* $G^* > 0$.

Proof. Let $P(0) > 0$. By the first equation in the immunological model (2.1), we obtain the following inequality:

$$P(\tau) \leq P(0)e^{\int_0^\tau [r-\delta G(s)]ds}. \tag{6.1}$$

Also note that if $M_0 > 0$ or $G_0 > 0$, then by comparison principle (similar argument to above), after some time, namely $\tilde{\epsilon}$, we obtain

$$G(\tau) \geq G(\tilde{\epsilon})e^{b\int_{\tilde{\epsilon}}^\tau P(s)ds} > 0. \tag{6.2}$$

By the way of contradiction assume that $\limsup_{\tau\to\infty} P(\tau) \neq 0$. Then the right hand side of the inequality (6.2) goes to infinity. Therefore $\lim_{\tau\to\infty} G(\tau) = \infty$. Then $\exists\tau^* : \forall\tau > \tau^*$, $G(\tau) > \frac{r}{\delta}$. Then as $\tau \to \infty$, the right handside of the inequality (6.1) goes to zero. It is a contradiction. Then $\lim_{\tau\to\infty} P(\tau) = 0$, subsequently $\lim_{\tau\to\infty} M(\tau) = 0$ and $\lim_{\tau\to\infty} G(\tau) = G^*$, for some $G^* > 0$. □

In summary, for any solution $(P(\tau), M(\tau), G(\tau))$ of the immunological model (2.1), with nonzero initial condition $(P(0), M(0), G(0))$, we have $\lim_{\tau\to\infty} P(\tau) = 0$, $\lim_{\tau\to\infty} M(\tau) = 0$, $\lim_{\tau\to\infty} G(\tau) = G^*$, where G^* is a positive real number and depends on the initial condition.

6.2. **Existence and Uniqueness of Equilibrium.**

Proof. (Proof of Theorem (2.1)) The proof is omitted. However, a sketch of the proof is as follows. It can be shown that the system is dissipative and asymptotically compact. In addition, the system is uniformly persistent when $\mathcal{R}_0 > 1$ (it is not hard to show that DFE is unstable when $\mathcal{R}_0 > 1$; then by a similar approach to Proposition 4.4 in [29], it can be shown that the system is uniform persistent). Then by [26], there exists at least one positive steady-state. Subsequently, by the argument of Proposition 3.1 in [14], it can be shown that this positive equilibrium has to be unique. The proof of local stability under the condition (2.5) is contained in the proof of $\mathcal{R}_0$ maximization in the next subsection. □

6.3. **Virus Evolution:$\mathcal{R}_0$ maximization.**

Proof. By taking $S_H(t) = S_H^* + x_H(t)$, $i_{H_1}(\tau, t) = i_{H_1}^*(\tau) + y_{H_1}(\tau, t)$, $i_{H_2}(\tau, t) = y_{H_2}(\tau, t)$, $R_H(t) = R_H^* + z_H(t)$, $S_V(t) = S_V^* + x_V(t)$, $I_{V_1}(t) = I_{V_1}^* + y_{V_1}(t)$, and $I_{V_2}(t) = y_{V_2}(t)$, we linearize the one host-two strain model (3.1) about the equilibrium $\mathcal{E}_1 = (S_H^*, i_{H_1}^*(\tau), 0, R_H^*, S_V^*, I_{V_1}^*, 0)$ and look for eigenvalues of the linear operator, that is we look for solutions of the form $x_H(t) = \overline{x}_H e^{\lambda t}, y_{H_1}(\tau, t) = \overline{y}_{H_1}(\tau)e^{\lambda t}, y_{H_2}(\tau, t) = \overline{y}_{H_2}(\tau)e^{\lambda t}, z_H(t) = \overline{z}_H e^{\lambda t}, x_V(t) = \overline{x}_V e^{\lambda t}, y_{V_1}(t) = \overline{y}_{V_1} e^{\lambda t}$, and $y_{V_2}(t) = \overline{y}_{V_2} e^{\lambda t}$, where $\overline{x}_H, \overline{y}_{H_1}, \overline{y}_{H_2}, \overline{z}_H, \overline{x}_V, \overline{y}_{V_1}$ and $\overline{y}_{V_2}$ are arbitrary nonzero constants (a function of τ in the case of y_{H_i}), but the eigenvalue λ is common. This process results in the following system (the bars have been ommitted):

(6.3)

$$
\begin{cases}
\lambda x_H &= \tilde{T}_0 \left(x_H + \sum_{i=1}^{2} \int_0^\infty (1 + \frac{\gamma_i(\tau)}{(\lambda+d)}) y_{H_i}(\tau) d\tau \right) \\
&\quad - \sum_{i=1}^{2} \beta_{v_i} S_H^* y_{V_i} - \beta_{v_1} x_H I_{V_1}^* - d x_H, \\
\frac{dy_{H_1}}{d\tau} + \lambda y_{H_1}(\tau) &= -\left(\alpha_1(\tau) + \kappa_1(\tau) + \gamma_1(\tau) + d\right) y_{H_1}(\tau), \\
y_{H_1}(0) &= \beta_{v_1} S_H^* y_{V_1} + \beta_{v_1} x_H I_{V_1}^*, \\
\\
\frac{dy_{H_2}}{d\tau} + \lambda y_{H_2}(\tau) &= -\left(\alpha_2(\tau) + \kappa_2(\tau) + \gamma_2(\tau) + d\right) y_{H_2}(\tau), \\
y_{H_2}(0) &= \beta_{v_2} S_H^* y_{V_2}, \\
\\
\lambda x_V &= -S_V^* \sum_{i=1}^{2} \int_0^\infty \beta_{h_i}(\tau) y_{H_i}(\tau) d\tau - x_V \sum_{i=1}^{2} \int_0^\infty \beta_{h_i}(\tau) i_{H_i}^*(\tau) d\tau - \mu x_V, \\
\lambda y_{V_1} &= S_V^* \int_0^\infty \beta_{h_1}(\tau) y_{H_1}(\tau) d\tau + x_V \int_0^\infty \beta_{h_1}(\tau) i_{H_1}^*(\tau) d\tau - \mu y_{V_1} \\
\lambda y_{V_2} &= S_V^* \int_0^\infty \beta_{h_2}(\tau) y_{H_2}(\tau) d\tau - \mu y_{V_2},
\end{cases}
$$

Note that by fourth and fifth equation in (6.3), we have $y_{H_2} = y_{H_2}(0) e^{-\lambda\tau} \pi_2(\tau)$, where $\pi_2(\tau) = e^{-\int_0^\tau (\alpha_2(s) + \kappa_2(s) + \gamma_2(s) + d)}$. Then rearranging the last equation in (6.3), we obtain

$$
y_{V_2} = \frac{S_V^* y_{H_2}(0) \int_0^\infty \beta_{h_2}(\tau) e^{-\lambda\tau} \pi_2(\tau) d\tau}{(\lambda + \mu)} \tag{6.4}
$$

Substituting (6.4) into the fifth equation (boundary condition for strain type 2), we obtain

$$
1 = S_V^* \beta_{v_2} S_H^* \int_0^\infty \beta_{h_2}(\tau) \frac{e^{-\lambda\tau}}{\lambda + \mu} \pi_2(\tau) d\tau. \tag{6.5}
$$

Suppose that $y_{V_2} \neq 0$, then the eigenvalues of the system will be determined by the characteristic equation $G(\lambda) = 1$, where $G(\lambda)$ is the right-hand side of the equation (6.5).

Note by the equilibrium condition, we have

$$
\frac{1}{S_V^* S_H^*} = \beta_{v_1} \int_0^\infty \beta_{h_1}(\tau) \frac{1}{\mu} \pi_1(\tau) d\tau, \tag{6.6}
$$

where $\pi_1(\tau) = e^{-\int_0^\tau (\alpha_1(s)+\kappa_1(s)+\gamma_1(s)+d)ds}$. Substituting (6.6) into (6.5), we obtain

$$G(\lambda) = \frac{\beta_{v_2}\int_0^\infty \beta_{h_2}(\tau)\frac{e^{-\lambda\tau}}{\lambda+\mu}\pi_2(\tau)d\tau}{\beta_{v_1}\int_0^\infty \beta_{h_1}(\tau)\frac{1}{\mu}\pi_1(\tau)d\tau} \tag{6.7}$$

Notice that $G(0) = \dfrac{\mathcal{R}_0^2}{\mathcal{R}_0^1}$, where $\mathcal{R}_0^i$ is reproduction number for strain type i. If $\mathcal{R}_0^2 > \mathcal{R}_0^1$, then $G(0) > 1$. Since $G(\lambda)$ is a decreasing function of λ,where λ is restricted to real numbers, and $\lim_{\lambda\to\infty} G(\lambda) = 0$, by intermediate value theorem, there exists a positive real number λ^* such that $G(\lambda^*) = 1$. Therefore if $\mathcal{R}_0^2 > \mathcal{R}_0^1$, then the strain-one equilibrium $\mathcal{E}_1$ is unstable.

Assume $\mathcal{R}_0^2 < \mathcal{R}_0^1$, that is $G(0) < 1$. Suppose that the system (6.3) has a solution $\lambda = a + ib$ such that $a \geq 0$. Then by the equation (6.5), we have

(6.8)
$$|G(\lambda)| = \left|S_V^*\beta_{v_2}S_H^*\int_0^\infty \beta_{h_2}(\tau)\frac{e^{-\lambda\tau}}{\lambda+\mu}\pi_2(\tau)d\tau\right| < \frac{S_V^*}{\mu}\beta_{v_2}S_H^*\int_0^\infty \beta_{h_2}(\tau)\pi_2(\tau)d\tau = G(0) < 1,$$

Hence, the characteristic equation $G(\lambda) = 1$ does not have solutions with nonnegative real part.

Now assume that $y_{V_2} = 0$. Then the stability of $\mathcal{E}_1$ depends on the eigenvalues of the following system:

$$\begin{cases} \lambda x_H = \tilde{T}_0\left(x_H + \int_0^\infty (1+\frac{\gamma_1(\tau)}{(\lambda+d)})y_{H_1}(\tau)d\tau\right) \\ \qquad\qquad -\beta_{v_1}S_H^*y_{V_1} - \beta_{v_1}x_H I_{V_1}^* - dx_H, \\ \frac{dy_{H_1}}{d\tau} + \lambda y_{H_1}(\tau) = -\left(\alpha_1(\tau)+\kappa_1(\tau)+\gamma_1(\tau)+d\right)y_{H_1}(\tau), \\ y_{H_1}(0) = \beta_{v_1}S_H^*y_{V_1} + \beta_{v_1}x_H I_{V_1}^*, \\ \\ \lambda x_V = -S_V^*\int_0^\infty \beta_{h_1}(\tau)y_{H_1}(\tau)d\tau - x_V\int_0^\infty \beta_{h_1}(\tau)i_{H_1}^*(\tau)d\tau - \mu x_V, \\ \lambda y_{V_1} = S_V^*\int_0^\infty \beta_{h_1}(\tau)y_{H_1}(\tau)d\tau + x_V\int_0^\infty \beta_{h_1}(\tau)i_{H_1}^*(\tau)d\tau - \mu y_{V_1}. \end{cases} \tag{6.9}$$

Since $y_{H_1}(\tau) = y_{H_1}(0)e^{-\lambda\tau}\pi_1(\tau)$, we have

$$\int_0^\infty (1+\frac{\gamma_1(\tau)}{(\lambda+d)})y_{H_1}(\tau)d\tau = (\beta_{v_1}S_H^*y_{V_1} + \beta_{v_1}x_H I_{V_1}^*)\int_0^\infty (1+\frac{\gamma_1(\tau)}{(\lambda+d)})e^{-\lambda\tau}\pi_1(\tau)d\tau.$$

Then the first equation in (6.9) is an equality in the terms of $x_H,\ y_{V_1}$ and λ obtained as follows:

$$x_H\left(\lambda+d-\tilde{T}_0+\beta_{v_1}I^*_{V_1}(1-\tilde{T}_0\int_0^\infty(1+\frac{\gamma_1(\tau)}{\lambda+d})e^{-\lambda\tau}\pi_1(\tau)d\tau)\right)$$
$$+y_{V_1}\beta_{v_1}S^*_H\left(1-\tilde{T}_0\int_0^\infty(1+\frac{\gamma_1(\tau)}{\lambda+d})e^{-\lambda\tau}\pi_1(\tau)d\tau\right)=0.$$

Also from the last two equations in (6.9) we obtain an equation in term of $x_H,\ y_{V_1}$ and λ.

$$y_{V_1}\left((\lambda+\mu+T_1)-\beta_{v_1}S^*_HS^*_V\int_0^\infty\beta_{h_1}(\tau)e^{-\lambda\tau}\pi_1(\tau)d\tau\right)$$
$$-x_H\left(S^*_V\beta_{v_1}I^*_{V_1}\int_0^\infty\beta_{h_1}(\tau)e^{-\lambda\tau}\pi_1(\tau)d\tau\right)=0,$$

where $T_1=\displaystyle\int_0^\infty\beta_{h_1}(\tau)i^*_{H_1}(\tau)d\tau(>0)$. The second equality is also in the terms of $x_H,\ y_{V_1}$ and λ. Then the characteristic equation is as follows:

$$\frac{\lambda+d+\beta_{v_1}I^*_{V_1}\hat{T}-\tilde{T}_0}{\lambda+d-\tilde{T}_0}=\frac{\beta_{v_1}S^*_HS^*_V\displaystyle\int_0^\infty\beta_{h_1}e^{-\lambda\tau}\pi_1(\tau)d\tau}{\lambda+\mu+T_1},$$

Suppose that $\lambda=a+bi$ with $a\geq 0$ is a solution of the characteristic equation. Taking the absolute value of both side of the equality above, we get

$$\left|\frac{\beta_{v_1}S^*_VS^*_H\displaystyle\int_0^\infty\beta_{h_1}(\tau)e^{-\lambda\tau}\pi_1(\tau)d\tau}{\lambda+\mu+T_1}\right|\leq\frac{\beta_{v_1}S^*_VS^*_H\displaystyle\int_0^\infty\beta_{h_1}(\tau)e^{-a\tau}\pi_1(\tau)d\tau}{\sqrt{(a+\mu+T_1)^2+b^2}}$$
$$\leq\frac{\beta_{v_1}S^*_VS^*_H\displaystyle\int_0^\infty\beta_{h_1}(\tau)e^{-a\tau}\pi(\tau)d\tau}{\mu}$$
$$\leq\beta_{v_1}\frac{S^*_V}{\mu}S^*_H\int_0^\infty\beta_{h_1}(\tau)\pi_1(\tau)d\tau=1$$

Moreover,

$$\left|\frac{\lambda+d+\beta_{v_1}I^*_{v_1}\hat{T}-\tilde{T}_0}{\lambda+d-\tilde{T}_0}\right|=\frac{\sqrt{(a+d+\beta_{v_1}I^*_{V_1}\Re\hat{T}-\tilde{T}_0)^2+(b+\beta_{v_1}I^*_{V_1}\Im\hat{T})^2}}{\sqrt{(a+d-\tilde{T}_0)^2+b^2}}.$$

Note that for λ with nonnegative real part, when $\Re\hat{T}\geq 0$ and $\Im\hat{T}\geq 0$ the left-hand side remains strictly greater than one, while the right-hand side is strictly smaller than one. Thus, such λ's cannot satisfy the characteristic equation (**??**). Hence the one strain endemic equilibrium $\mathcal{E}_1$ is locally asymptotically stable whenever it exists given the assumptions on $\hat{T}$. We notice that the conditions $\Re\hat{T}\geq 0$ and $\Im\hat{T}\geq 0$ for any λ with $\Re\lambda\geq 0$ may not always hold. □

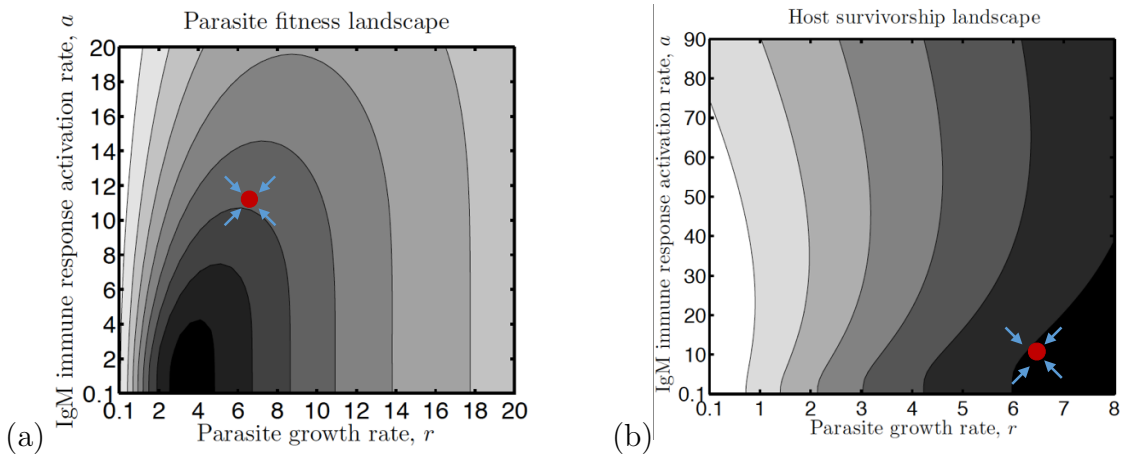

FIGURE 9. Host and parasite fitness landscape across distinct immune activation rate a and parasite growth rate r and the coevolutionary attractor $(a^*_{CoESS}, r^*_{CoESS})$.

SCHOOL OF BIOLOGICAL SCIENCES AND SCHOOL OF MATHEMATICS, GEORGIA INSTITUTE OF TECHNOLOGY, 310 FERST DR., ATLANTA, GA 30332
E-mail address: Hayriye.Gulbudak@asu.edu

DEPARTMENT OF BIOLOGY, UNIVERSITY OF FLORIDA, 220 BARTRAM HALL, PO BOX 118525, GAINESVILLE, FL 32611–8525
E-mail address: vcannataro@ufl.edu

DEPARTMENT OF MATHEMATICAL SCIENCES, FLORIDA ATLANTIC UNIVERSITY, SCIENCE BUILDING, ROOM 234 777 GLADES ROAD BOCA RATON, FL 33431
E-mail address: ntuncer@fau.edu

DEPARTMENT OF MATHEMATICS, UNIVERSITY OF FLORIDA, 358 LITTLE HALL, PO BOX 118105, GAINESVILLE, FL 32611–8105
E-mail address: maia@math.ufl.edu